

## Article

# Using Wavelet Analysis to Examine Long-Term Variability of Phytoplankton Biomass in the Tropical, Saline Lake Alchichica, Mexico

Javier Alcocer <sup>1,\*</sup>, Benjamín Quiroz-Martínez <sup>2</sup>, Martín Merino-Ibarra <sup>3</sup>, Luis A. Oseguera <sup>1</sup> and Miroslav Macek <sup>1</sup>

<sup>1</sup> Grupo de Investigación en Limnología Tropical, Facultad de Estudios Superiores Iztacala, Universidad Nacional Autónoma de México, Tlalnepantla 54090, Mexico; [loseguera@unam.mx](mailto:loseguera@unam.mx) (L.A.O.); [mirek@unam.mx](mailto:mirek@unam.mx) (M.M.)

<sup>2</sup> Laboratorio de Ecología Numérica y Análisis de Datos, Instituto de Ciencias del Mar y Limnología, Universidad Nacional Autónoma de México, Av. Universidad 3000, Ciudad de México 04510, Mexico; [bquirozm@cmarl.unam.mx](mailto:bquirozm@cmarl.unam.mx)

<sup>3</sup> Unidad Académica de Ecología y Biodiversidad Acuática, Instituto de Ciencias del Mar y Limnología, Universidad Nacional Autónoma de México, Av. Universidad 3000, Ciudad de México 04510, Mexico; [mmmerino@cmarl.unam.mx](mailto:mmmerino@cmarl.unam.mx)

\* Correspondence: [jalcocer@unam.mx](mailto:jalcocer@unam.mx)



**Citation:** Alcocer, J.; Quiroz-Martínez, B.; Merino-Ibarra, M.; Oseguera, L.A.; Macek, M. Using Wavelet Analysis to Examine Long-Term Variability of Phytoplankton Biomass in the Tropical, Saline Lake Alchichica, Mexico. *Water* **2022**, *14*, 1346. <https://doi.org/10.3390/w14091346>

Academic Editors: Nickolai Shadrin, Gonzalo Gajardo and Elena Anufrieva

Received: 11 March 2022

Accepted: 18 April 2022

Published: 21 April 2022

**Publisher's Note:** MDPI stays neutral with regard to jurisdictional claims in published maps and institutional affiliations.



**Copyright:** © 2022 by the authors. Licensee MDPI, Basel, Switzerland. This article is an open access article distributed under the terms and conditions of the Creative Commons Attribution (CC BY) license (<https://creativecommons.org/licenses/by/4.0/>).

**Abstract:** The phytoplankton biomass (chlorophyll-a, Chl-a) is directly related to the total production of lakes. Chl-a in temperate lakes oscillates on an annual scale. However, Chl-a oscillations in tropical lakes have hardly been documented, particularly over multiple years. Here, we described the periodicity of the Chl-a by performing a continuous wavelet analysis of 21 years (1998–2018), monthly Chl-a data from tropical, saline Lake Alchichica, Mexico. Parallel wavelet analyses were made on environmental time series (i.e., euphotic zone, mixed layer, temperature, dissolved oxygen concentration, dissolved inorganic nitrogen, soluble reactive phosphorus, soluble reactive silica). Throughout the time series, the wavelet transforms identified a regular and predictable annual cycle of the Chl-a associated with the warm-monomictic thermal-mixing pattern, the variability of the annual Chl-a cycle, and the presence of other cyclicities, 2-year and ~4–5 years, associated with external forcing agents (e.g., North Pacific Oscillation). The water quality variables display a recurrent annual cycle. At the same time, the trophic variables (nutrient concentration) showed the same cyclicity as Chl-a (1-year, 2-year, and 4-year), suggesting the external forcing agents promote Chl-a augment through nutrient increase made available from stronger, deeper, mixing periods.

**Keywords:** wavelet analysis; chlorophyll-a; warm monomixis; nutrients; oligotrophic

## 1. Introduction

Phytoplankton biomass, expressed as chlorophyll-a (Chl-a), is directly related to the total production of lakes [1] and can be used as a proxy for primary production [2]. Spatial and temporal changes in Chl-a are primarily controlled by light, temperature, and nutrients in the water column. These factors also determine the phytoplankton's size spectrum and species composition [3,4]. The annual phytoplankton succession was well documented in deep, thermally stratified temperate lakes (the Plankton Ecology Group model, e.g., [5,6]), with a unimodal phytoplankton maximum in the spring in oligotrophic lakes due to nutrient limitation.

Although many studies examined the phytoplankton variability within years, and more recently, a few long-term phytoplankton data are becoming available, few studies encompass datasets of several years or decades, primarily due to the lack of data [7]. The absence of long-term phytoplankton data and lack of continuity in records is common for tropical lakes [8,9]. According to Talling [10], the annual patterns of phytoplankton

seasonality in the tropical belt are dominated by hydrological features (water inputs–outputs) or by hydrographic ones (water-column structure and circulation). Lewis [11] mentioned that in tropical lakes, the changes in phytoplankton abundance could be driven autogenically, as the organisms modify their environment (e.g., through nutrient uptake) or allogenically, associated with abiotic influences (e.g., water column mixing). Phytoplankton biomass in large tropical lakes varies at different time scales from seasons to centuries [12]. The seasonal scale in the tropics is driven by the alternation between the rainy (warm) and dry (cold) periods. In contrast, the global climate (e.g., El Niño Southern Oscillation, the Pacific Decadal Oscillation) drives the long-term scale. Despite the apparent “endless summer” [13] in tropical inland waters, there is commonly one event of deep water-column mixing, but also other different time-variability patterns (period/frequency and amplitude/range) such as the diel (24 h) cycle, the annual cycles with other periodicities (lunar, seiches, sunspots), and long-term and aperiodic or non-seasonal environmental changes [4,14].

Annual phytoplankton patterns differ across ecosystems, have large year-to-year variability [15–17], and are not strongly expressed in all aquatic ecosystems [18,19]. Whereas high variability of seasonal phytoplankton patterns is documented, no systematic analysis of annual cycles has been conducted to identify their characteristic periods of biomass variability and the recurrence strength at those periods [20].

Wavelet analysis performs a time-frequency analysis of the signal, which permits the estimation of the spectral characteristics of the signal as a function of time [21] and then the identification of different periodic components and their time evolution all along with the time series. Wavelet transforms are useful tools for determining the dominant scales of variation in time series and are used to examine periodicities in plankton communities [15,18,20]. However, this approach has been scarcely applied in tropical limnology.

In this work, our main goal was to reveal the variability in the annual periodicity of the phytoplankton Chl-a over 21 years and relate the variability with the environmental variables in the tropical saline Lake Alchichica, Puebla, Mexico. For this purpose, we addressed the following research questions: What are the cyclicity periods throughout 21 years (1998–2018) of (1) water quality and trophic status and (2) Phytoplankton Chl-a?

Our working hypothesis was that in this tropical, saline lake, the warm-monomictic thermal mixing pattern is the key factor determining the phenology of the pelagic Chl-a concentration. Specifically, we expected (1) to identify a predictable and recurrent annual cycle and (2) to unravel longer-term cyclicity. In order to answer the research questions and test the proposed hypothesis, our approach was to evaluate the temporal, long-term changes using data derived from monthly monitoring of the water column for 21 years (1998–2018) in the (a) water quality and trophic status and (b) phytoplankton Chl-a.

## 2. Materials and Methods

### 2.1. Study Area

Lake Alchichica is a volcanic maar in Puebla State ( $19^{\circ}24.7' N$ ,  $97^{\circ}24.0' W$ , 2300 m above the sea level), at the easternmost portion of the Mexican Plateau [22] (Figure 1).

The climate is temperate and semi-arid with an average temperature of  $12.9^{\circ}C$ , rainfall  $< 500 \text{ mm year}^{-1}$ , concentrated in the (“summer”) rainy season, and evapotranspiration rate up to  $1690 \text{ mm year}^{-1}$  [3]. It is a deep lake (maximum depth 62 m, mean depth 40.9 m), circular in shape (maximum length 1902 m), with a surface area of  $2.367 \text{ km}^2$ , a shoreline of 5.84 km, and a volume of  $114,688,900 \text{ m}^3$  [23]. The lake is saline (total dissolved solids =  $10.08 \text{ g L}^{-1}$ , electrical conductivity =  $13.53 \text{ mS cm}^{-1}$ ) with chloride, bicarbonate, sodium, and magnesium as dominant ions and an alkaline pH (8.7–9.2) [22,24]. Alchichica is a warm monomictic lake that circulates during the cold, dry season, from the end of December or the beginning of January to the end of March or the beginning of April. The lake remains stratified throughout the warm rainy season, and the hypolimnion becomes anoxic for most of this period [22]. Lake Alchichica is oligotrophic with an overall nutrient concentration of  $< 4 \mu\text{mol L}^{-1}$  at the mixed layer [25].

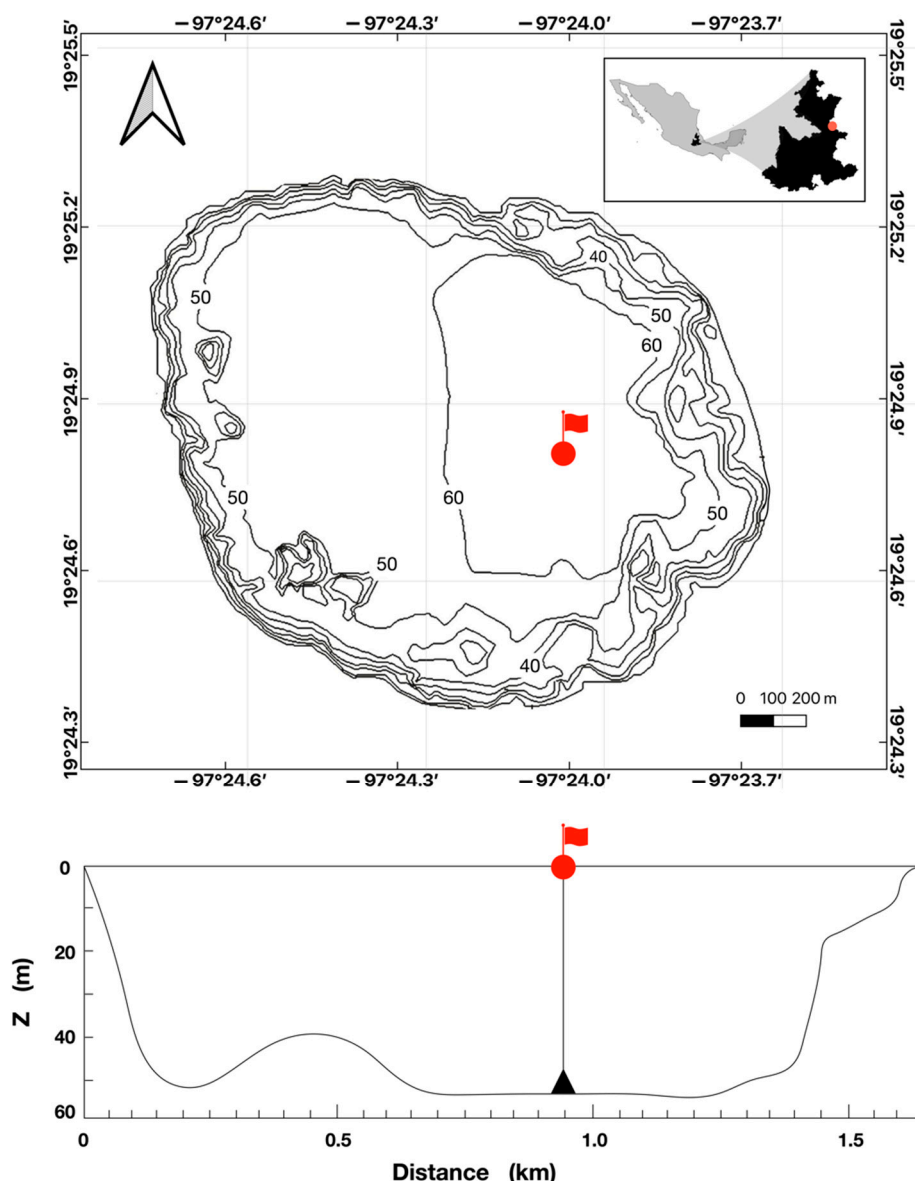


**Figure 1.** Bathymetric map of Lake Alchichica (**up**). Location in Mexico and Puebla State. Isobaths in meters. Bathymetric profile (**down**). The red buoy indicates the sampling station.

Nineteen species compose the phytoplankton community in Lake Alchichica, with diatoms the most diverse group with ten species. The annual phytoplankton dynamics display three characteristic features: (1) a winter diatom bloom during the mixing season, (2) a cyanobacterial bloom at the onset of the stratification period, and (3) a deep chlorophyll maximum (DCM) along the stratification period [26].

The phytoplankton biomass in Lake Alchichica is dominated (>70%) by large-sized individuals [3] corresponding to *Cyclotella alchichicana* Oliva, Lugo, Alcocer and Cantoral-Uriza, 2006; *C. choctawhatcheeana* Prasad, 1990; *Chaetoceros elmorei* Boyer, 1914; and *Nodularia aff. spumigena* Mertens ex Bornet and Flahault, 1888). Among these species, the large (35–63 µm in diameter) diatom *C. alchichicana* [27] comprised most of the phytoplankton biomass. It dominated the winter diatom bloom and the DCM during the stratification period, except for a brief period at the onset of the stratification when *Nodularia aff. spumigena* bloomed [28].

## 2.2. Physical, Chemical, and Chl-a Characterisation

The long-term database herein analyzed comprises a monthly sampling program made over 21 years (1998–2018) for Chl-a, euphotic zone, temperature, and dissolved oxygen in the mixed layer, and over 20 years (1999–2018) for nutrients. All samplings were made at the same station, located in the central and deepest part of the lake, and at the same time (12–13 h).

Vertical photosynthetically active radiation (PAR) and natural fluorescence profiles were recorded with a Biospherical natural fluorescence profiler model PNF-300. The profiles consisted of discrete readings recorded every second as the sensor was lowered at about 1 m per 3–4 s, providing a vertical resolution of 25–30 cm. PAR profiles were used to identify the depth of the euphotic zone ( $Z_{EU} = 0.1\%$  surface PAR). Vertical water temperature and dissolved oxygen profiles were recorded with water quality monitoring probes (Hydrolab Datasonde models DS3, DS4, or DS5) with a vertical resolution of 1 m. Temperature and dissolved oxygen (DO) profiles were used to recognize the main stages of the lake's thermal regime (stratification and mixing) and to identify the depth of the mixed layer ( $Z_{MIX}$ ).

Chlorophyll-a concentration ( $\text{mg m}^{-3}$ ) was calculated from the natural fluorescence flux,  $F_f$ , and the incident irradiance. The natural fluorescence of Chl-a is defined as the total flux of light emitted by Chl-a in a suspension of phytoplankton per unit volume under ambient light. Keifer et al. [29] and Chamberlain et al. [30] showed that measurements of natural fluorescence flux ( $F_f$ ) and scalar irradiance of PAR ( $E_o$  (PAR)) provide accurate estimates of Chl-a.

$$\text{Chl-a} = F_f \div {}^o a_c (\text{PAR}) \times \varphi_f \times E_o (\text{PAR})$$

The natural fluorescence records of the first five surface meters were omitted since the algorithms (from the profiler software) used to calculate the concentration of Chl-a from the natural fluorescence interpret that all the flow of red light directed upwards comes from Chl-a fluorescence. However, near the water's surface (the first five meters in transparent waters such as Alchichica), this interpretation is incorrect due to the dispersion of the red wavelength [29].

There are two important optical assumptions used in this:  ${}^o a_c$  (PAR) is the chlorophyll-specific absorption coefficient (absorption normalized to chlorophyll concentration), and  $\varphi_f$  is the quantum yield of fluorescence. These values are treated as constants in the software for the PNF-300 with values of  $0.04 \text{ m}^2 \text{ mg}^{-1}$  and  $0.045 \text{ mE}$  fluoresced per mE absorbed, respectively. The Chl-a concentration profiles were integrated per unit area ( $\text{m}^2$ ) to calculate the total Chl-a concentration per  $\text{m}^2$ .

Ten water samples along the vertical profile were obtained for nutrient analysis at each sampling date (5-L Uwitec water sampler bottle). Water samples were filtered through mixed cellulose esters syringe filters (0.22- $\mu\text{m}$  pore, Millex, Millipore, Ireland), collected in polypropylene containers, and stored frozen until analysis (within 48 h). Analyses of dissolved inorganic nitrogen ( $\text{DIN} = \text{NH}_4^+ + \text{NO}_2^- + \text{NO}_3^-$ ), soluble reactive phosphorus (SRP), and soluble reactive silica (SRSi) used a segmented-flow Autoanalyzer (Skalar San Plus System, Skalar Analytical B.V., Breda, The Netherlands) following Hansen and Koroleff [31].

Before wavelet analysis, we performed a seasonally-adjusted Mann–Kendall Trend Test to account for any seasonality in the phytoplanktonic chlorophyll-a concentration (1998–2018), water quality (1998–2018), and trophic (1999–2018) variables of Lake Alchichica. Analyses were run in R-4.0.3 [32].

## 2.3. Wavelet Analysis

Wavelet analysis used continuous wavelet transforms to determine the dominant scales of variability for Chl-a, physical and chemical time series from 1998 to 2018 as a function of period and time. Wavelet analysis emerged as a tool for characterizing periodicities in non-stationary time series, as it decomposes a time series in both the frequency and time domains [33]. The latter is why it has become an important tool to analyze time series since it performs a time-frequency analysis of a signal, allowing the

estimation of the spectral characteristics of the signal as a function of time [21,34], and at the same time, identifies the different periodic components and their time evolution over time. The use of wavelet analysis in aquatic ecology has increased over the last few years, especially in marine ecology. Wavelet transforms are useful tools for determining the dominant scales of variation in time series and are increasingly used to examine the periodicities in plankton (e.g., [15,20]) and other aquatic communities. Wavelet analysis performs a time-scale decomposition of the signal by estimating its frequency characteristics as a function of time [20,35].

The continuous Morlet wavelet transform was used to normalize monthly time series data and obtain the wavelet power spectrum of the time series. The wavelet power spectrum identifies the periods that are the most important sources of variability across time. In addition, it is possible to obtain a global wavelet spectrum, which is similar to Fourier spectra, that identifies the variance associated with each period for a given time series [33]. Due to the nature of the data, the original time series is not equally spaced and was made regular using spline interpolation. All the analyses for spline interpolations and wavelet transforms were performed using Matlab.

### 3. Results

#### 3.1. Chlorophyll-a

We observed substantial variability in the Chl-a concentration in Lake Alchichica throughout 1998–2018 with three extremes ( $>50 \text{ mg m}^{-2}$ ) peaks: October–November 2003, October 2009, and August–September 2015 (Figure 2). The Chl-a concentration annual average was  $23 \pm 4 \text{ mg m}^{-2}$  within  $18 \pm 4 \text{ mg m}^{-2}$  and  $30 \pm 13 \text{ mg m}^{-2}$ . There was a linearly decreasing trend in the Chl-a concentration from 1998 to 2018.

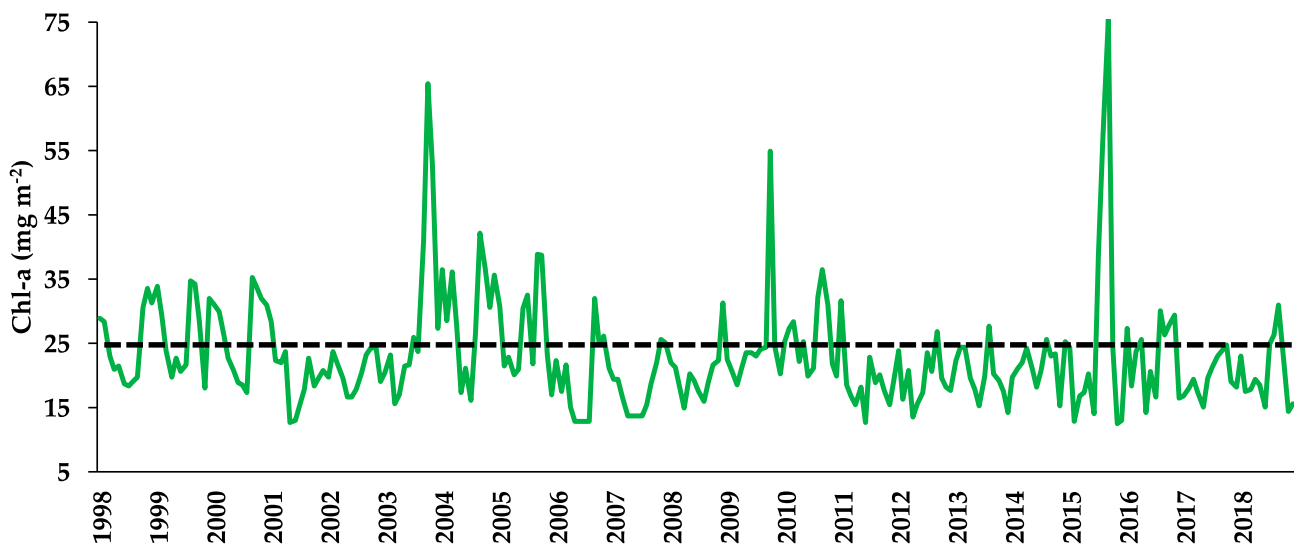


**Figure 2.** Temporal dynamics of the water-column integrated chlorophyll-a concentration (Chl-a) in Lake Alchichica. (The dashed line indicates the average Chl-a value from 1998 to 2018).

The Chl-a concentration fluctuated interannually (Figure 3). For 48% of the period, the Chl-a concentration was above the annual average, while 52% was below the annual average. The above and below the average Chl-a concentration regularly alternated (three above, two below, three above, three below, two above, four below, two above, two below). Annually, Chl-a concentration displayed a regular dynamic with two peaks (Figure 3). The first peak was associated with the winter (January to March) mixing period when diatoms bloom throughout the water column. The second peak was related to developing a DCM at the metalimnion during the stratification reaching maximum concentrations in September–October.

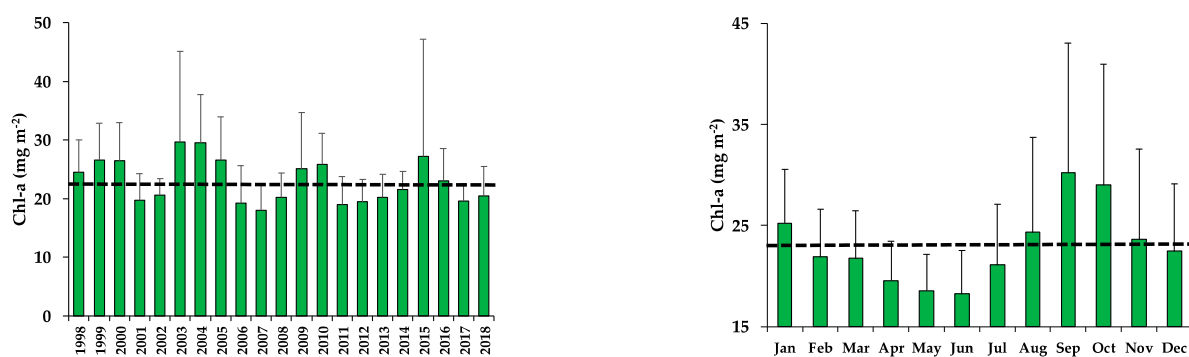


**Figure 3.** Interannual (left) and annual (seasonal) (right) variation in the water-column integrated chlorophyll-a concentration (Chl-a) in Lake Alchichica. (The dashed lines indicate the average Chl-a value from 1998 to 2018).

### 3.2. Euphotic Zone ( $Z_{EU}$ )

There was interannual variability in the euphotic zone ( $Z_{EU}$ ) of Lake Alchichica from 1998 to 2018 (Figure 4). A recurrent annual pattern evidences the turbid and the clear water phases. There was a linearly decreasing trend in the  $Z_{EU}$  from 1998 to 2018. The  $Z_{EU}$  annual average was  $31 \pm 6$  m within  $27 \pm 6$  m and  $37 \pm 8$  m.

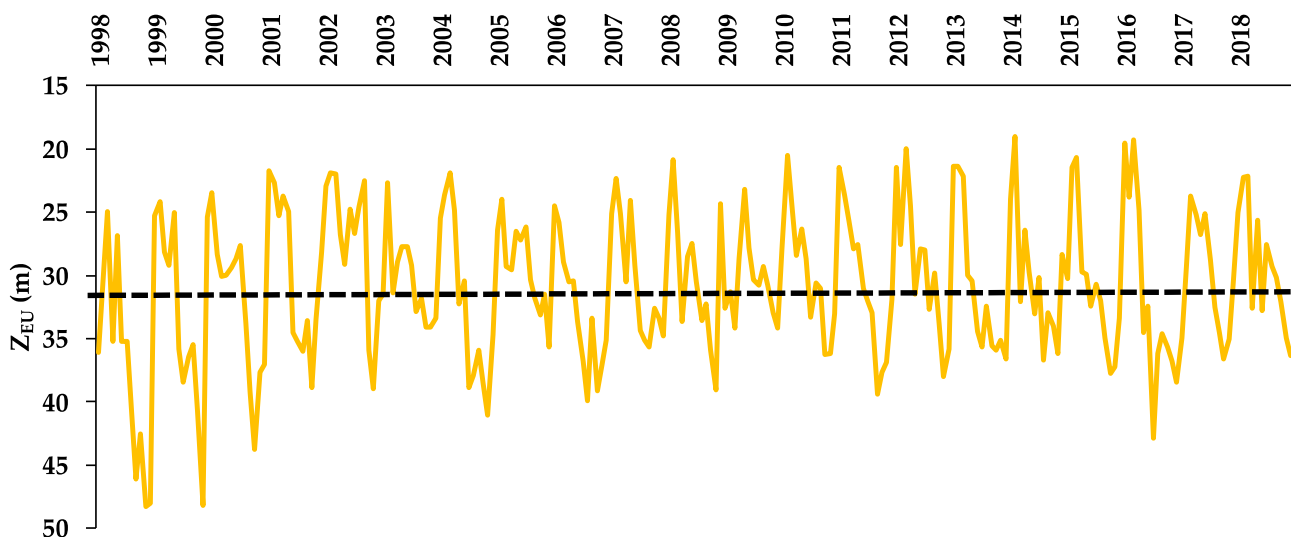


**Figure 4.** Temporal dynamics of the euphotic zone ( $Z_{EU}$ ) in Lake Alchichica. (The black dashed line indicates the average  $Z_{EU}$  value from 1998 to 2018).

The  $Z_{EU}$  fluctuated interannually (Figure 5). For 29%, the  $Z_{EU}$  was above the annual average, while for 71%, it was below the annual average. The  $Z_{EU}$  displayed a regular dynamic with two phases annually (Figure 5). The first is the turbid water phase with  $Z_{EU}$  below the annual average (31 m) during the mixing and early stratification (January to June). For the second one, the clear water phase with  $Z_{EU}$  was above the annual average during the well-established and late stratification (July to December).

### 3.3. Mixed Layer Depth ( $Z_{MIX}$ )

The mixed layer depth ( $Z_{MIX}$ ) displayed interannual variability in Lake Alchichica from 1998 to 2018 (Figure 6). A recurrent annual pattern evidences the water column mixing and stratification periods. The  $Z_{MIX}$  annual average was  $29 \pm 10$  m within  $24 \pm 16$  m and  $34 \pm 21$  m. There was a linearly decreasing trend in the  $Z_{MIX}$  from 1998 to 2018.

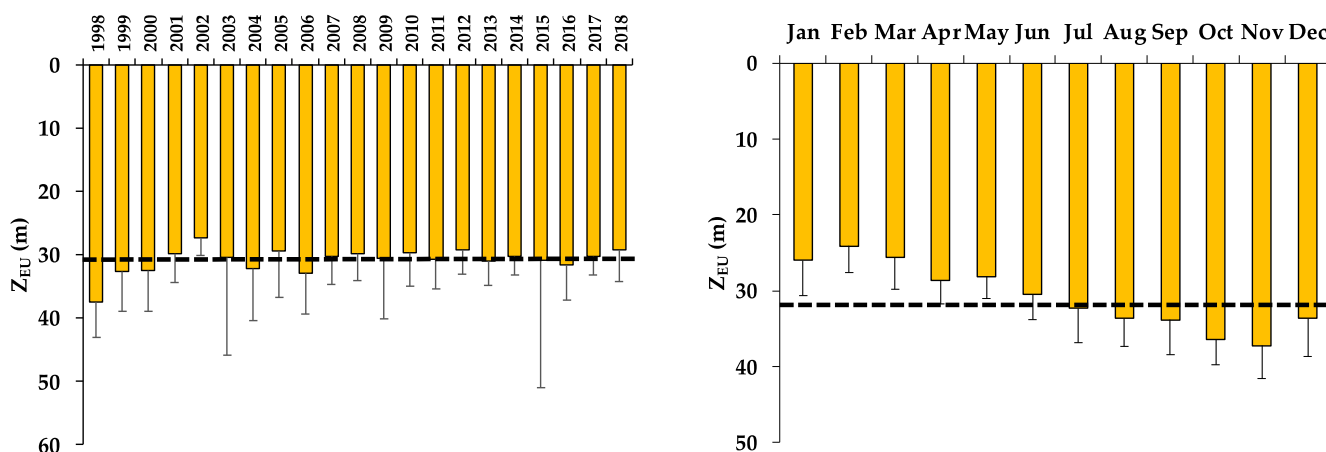


**Figure 5.** Interannual (left) and annual (seasonal) (right) variation (average  $\pm$  s.d.) in the euphotic zone ( $Z_{EU}$ ) in Lake Alchichica. (The dashed lines indicate the average  $Z_{EU}$  value from 1998 to 2018).

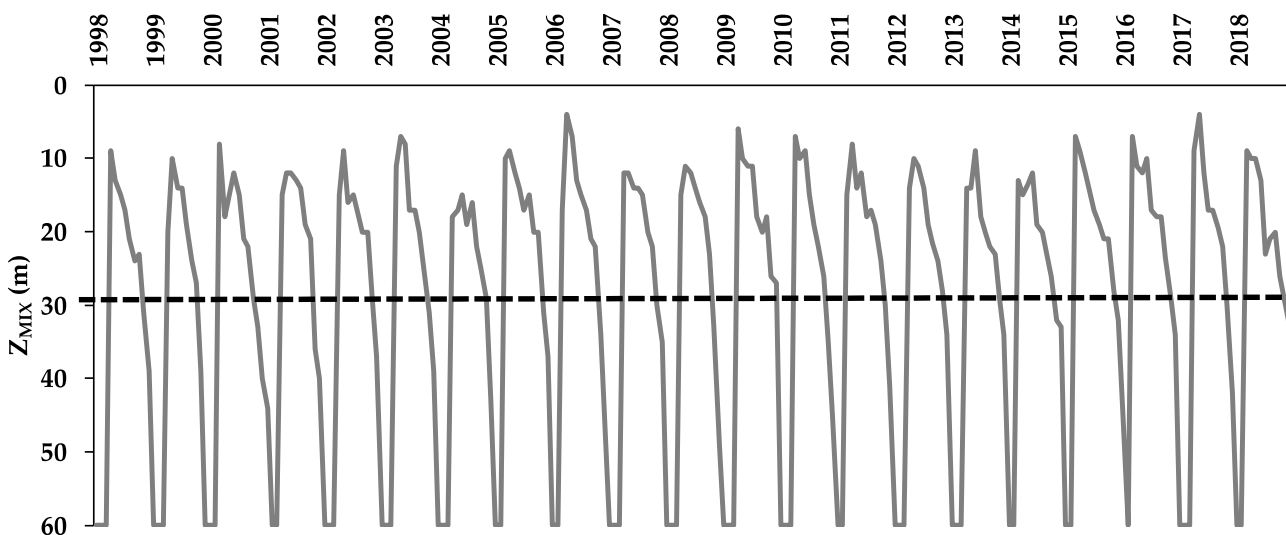


**Figure 6.** Temporal dynamics of the mixed layer ( $Z_{MIX}$ ) in Lake Alchichica. (The black dashed line indicates the average  $Z_{MIX}$  value from 1998 to 2018).

The  $Z_{MIX}$  fluctuated interannually (Figure 7). For 52% of the period, the  $Z_{MIX}$  was above the annual average, while 48% was below the annual average. Annually, the  $Z_{MIX}$  displayed a regular dynamic with two seasons. The first is when  $Z_{MIX}$  is maximum (i.e., the whole water column) during the winter mixing period (January to March). The second one corresponded to the extended stratification season (April to December). The  $Z_{MIX}$  decreased rapidly in April at the onset of the stratification and from then on increased gradually along with the well-established and late stratification. The  $Z_{MIX}$  was above the annual average from January to March and November to December and below the average from April to October (Figure 7).

#### 3.4. Temperature of the Mixed Layer ( $T_{MIX}$ )

The mixed layer temperature ( $T_{MIX}$ ) displayed interannual variability in Lake Alchichica from 1998 to 2018 (Figure 8). A recurrent annual pattern evidences the cold/dry and the warm/rainy seasons associated with the tropical climate. The  $T_{MIX}$  annual average was  $17.4 \pm 1.8$  °C within a range of  $16.9 \pm 1.7$  °C and  $18.2 \pm 1.8$  °C. There was an increasing linear trend in the  $T_{MIX}$  from 1998 to 2018.

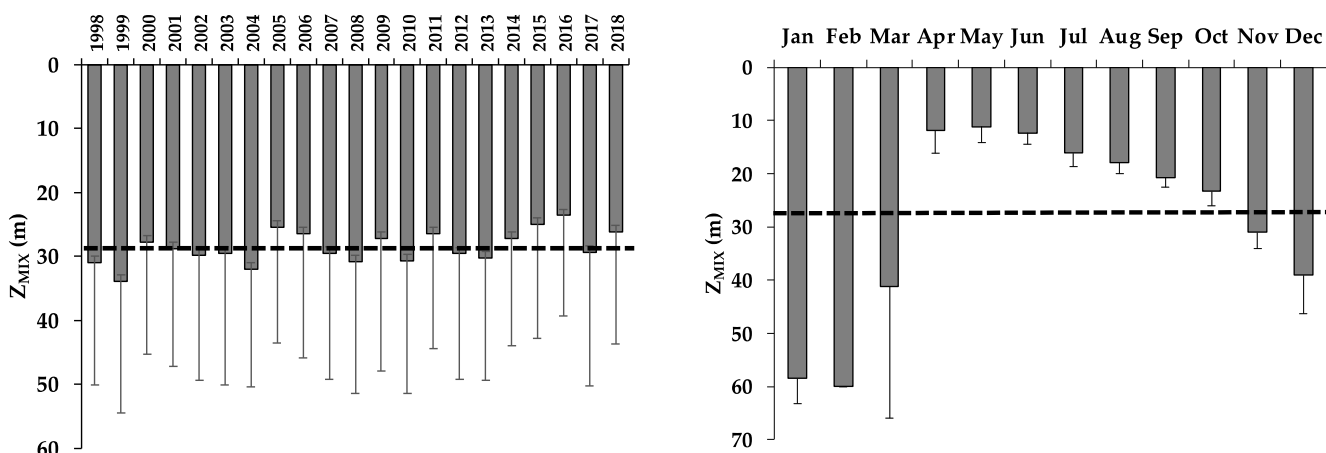


**Figure 7.** Interannual (left) and annual (seasonal) (right) variation (average  $\pm$  s.d.) in the mixed layer ( $Z_{\text{MIX}}$ ) in Lake Alchichica. (The dashed lines indicate the average  $Z_{\text{MIX}}$  value from 1998 to 2018).

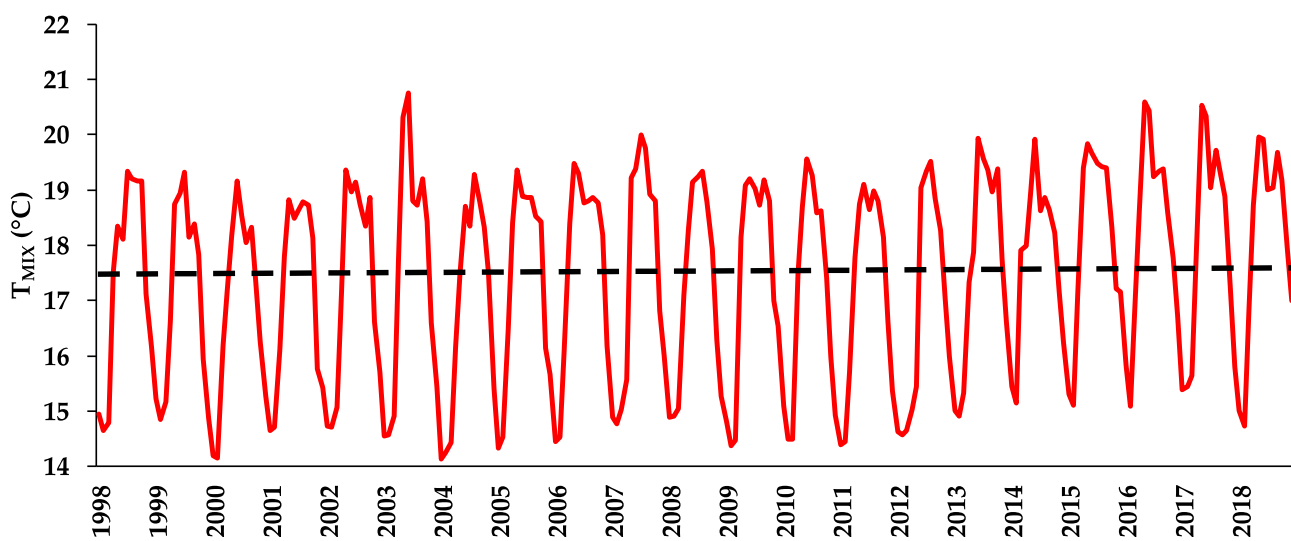


**Figure 8.** Temporal dynamics of the temperature in the mixed layer ( $T_{\text{MIX}}$ ) in Lake Alchichica. (The black dashed line indicates the average  $T_{\text{MIX}}$  value from 1998 to 2018).

The  $T_{\text{MIX}}$  fluctuated interannually (Figure 9). For 48% of the period, the  $T_{\text{MIX}}$  was above the annual average, while 52% was below the annual average. The  $T_{\text{MIX}}$  displayed a regular dynamic with two periods (Figure 9). The first was when  $T_{\text{MIX}}$  was colder (below the average) during the winter and late stratification (January–March, and November–December). The second one corresponded to the well-established and late stratification season (April to October) when  $T_{\text{MIX}}$  was warmer (above the average).

### 3.5. Dissolved Oxygen of the Mixed Layer ( $DO_{\text{MIX}}$ )

The dissolved oxygen concentration of the mixed layer ( $DO_{\text{MIX}}$ ) displayed interannual variability in Lake Alchichica from 1998 to 2018 (Figure 10). A recurrent annual pattern evidences the water column mixing and stratification periods. The  $DO_{\text{MIX}}$  annual average was  $6.3 \pm 1.0 \text{ mg L}^{-1}$  within  $5.6 \pm 1.1 \text{ mg L}^{-1}$  and  $6.9 \pm 0.9 \text{ mg L}^{-1}$ . There was an increasing linear trend in the  $DO_{\text{MIX}}$  from 1998 to 2018.

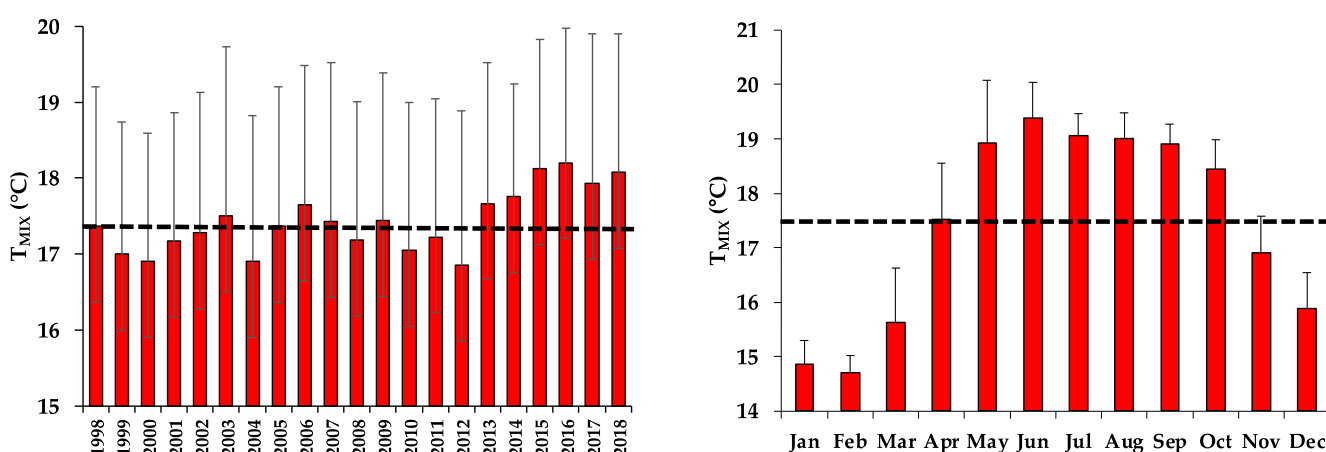


**Figure 9.** Interannual (left) and annual (seasonal) (right) variation in the temperature (average  $\pm$  s.d.) in the mixed layer ( $T_{MIX}$ ) in Lake Alchichica. (The dashed lines indicate the average  $T_{MIX}$  value from 1998 to 2018).

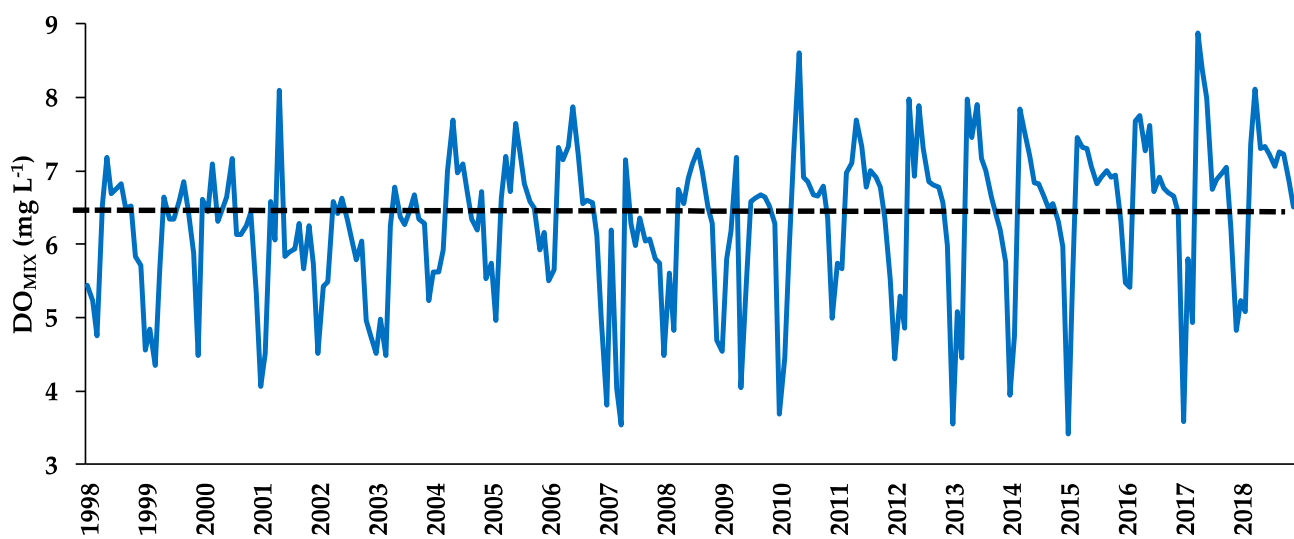


**Figure 10.** Temporal dynamics of the dissolved oxygen concentration in the mixed layer ( $DO_{MIX}$ ) in Lake Alchichica. (The black dashed line indicates the average  $DO_{MIX}$  value from 1998 to 2018).

The  $DO_{MIX}$  fluctuated interannually (Figure 11). For 57% of the period, the  $DO_{MIX}$  was above the annual average, while 43% was below the annual average. The  $DO_{MIX}$  displayed a regular seasonal dynamic with two periods (Figure 11). The first was when  $DO_{MIX}$  was lower (below the annual average) during the winter and late stratification (January–March and November–December). The second one corresponded to the well-established and late stratification season (April to October) when  $DO_{MIX}$  was higher (above the annual average). The reduction in  $DO_{MIX}$  takes place from the late stratification (through the erosion of the thermocline) to the mixing period when the anoxic hypolimnetic water mixes with the aerobic epilimnetic waters.

### 3.6. Dissolved Inorganic Nitrogen of the Mixed Layer ( $DIN_{MIX}$ )

The dissolved inorganic nitrogen concentration in the mixed layer ( $DIN_{MIX}$ ) displayed substantial interannual variability in Lake Alchichica from 1999 to 2018 (Figure 12). There was no clear annual pattern of  $DIN_{MIX}$  associated with the water column mixing and stratification periods. The  $DIN_{MIX}$  annual average was  $2.7 \pm 2.0\ \mu M$  within a range of  $1.1 \pm 0.5\ \mu M$  and  $5.1 \pm 3.4\ \mu M$ . There was an increasing linear trend in the  $DIN_{MIX}$  from 1999 to 2018.

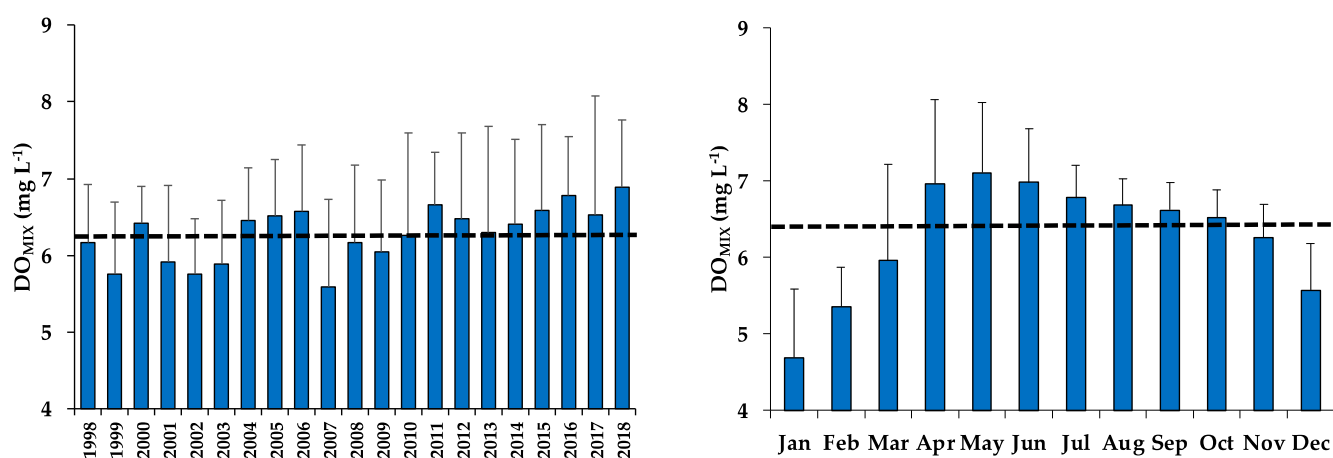


**Figure 11.** Interannual (left) and annual (seasonal) (right) variation in the dissolved oxygen concentration (average  $\pm$  s.d.) in the mixed layer (DO<sub>MIX</sub>) in Lake Alchichica. (The dashed lines indicate the average DO<sub>MIX</sub> value from 1998 to 2018).

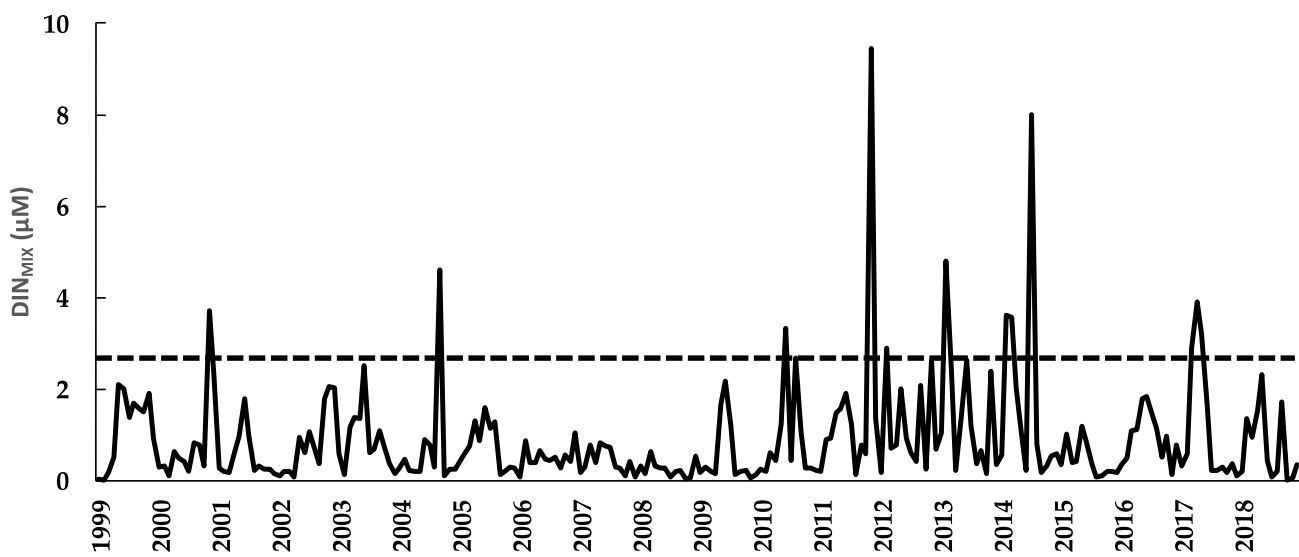


**Figure 12.** Temporal dynamics of the dissolved inorganic nitrogen concentration in the mixed layer (DIN<sub>MIX</sub>) in Lake Alchichica. (The black dashed line indicates the average DIN<sub>MIX</sub> value from 1998 to 2018).

The DIN<sub>MIX</sub> fluctuated interannually (Figure 13). For 45% of the period, the DIN<sub>MIX</sub> was above the annual average, while 55% was below the annual average. The DIN<sub>MIX</sub> displayed a regular dynamic with two periods (Figure 13). The first was when DIN was lower (below the annual average) at the onset and along most of the stratification (April, June to October, and December). The second one corresponded primarily to the mixing season (January to March), May, and November, when DIN was higher (above the annual average).

### 3.7. Soluble Reactive Phosphorus of the Mixed Layer (SRP<sub>MIX</sub>)

The soluble reactive phosphorous concentration in the mixed layer (SRP<sub>MIX</sub>) displayed substantial interannual variability in Lake Alchichica from 1999 to 2018 (Figure 14). There was no clear annual pattern of the SRP<sub>MIX</sub> associated with the water column mixing and stratification periods. The SRP<sub>MIX</sub> annual average was  $0.27 \pm 0.16 \mu\text{M}$  within a range of  $0.15 \pm 0.11 \mu\text{M}$  and  $0.53 \pm 0.24 \mu\text{M}$ .

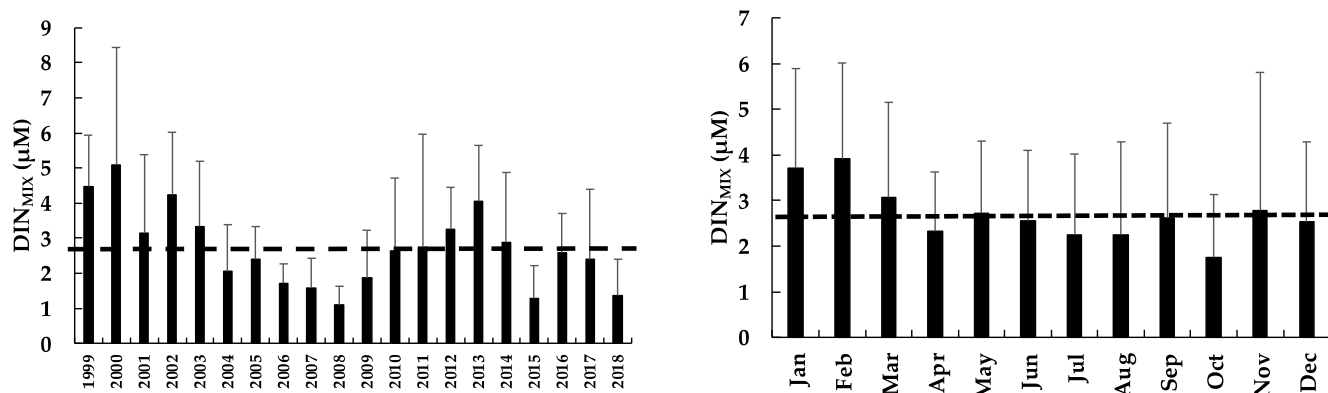


**Figure 13.** Interannual (left) and annual (seasonal) (right) variation in the dissolved inorganic nitrogen concentration (average  $\pm$  s.d.) in the mixed layer (DIN<sub>MIX</sub>) in Lake Alchichica. (The dashed lines indicate the average DIN<sub>MIX</sub> value from 1998 to 2018).

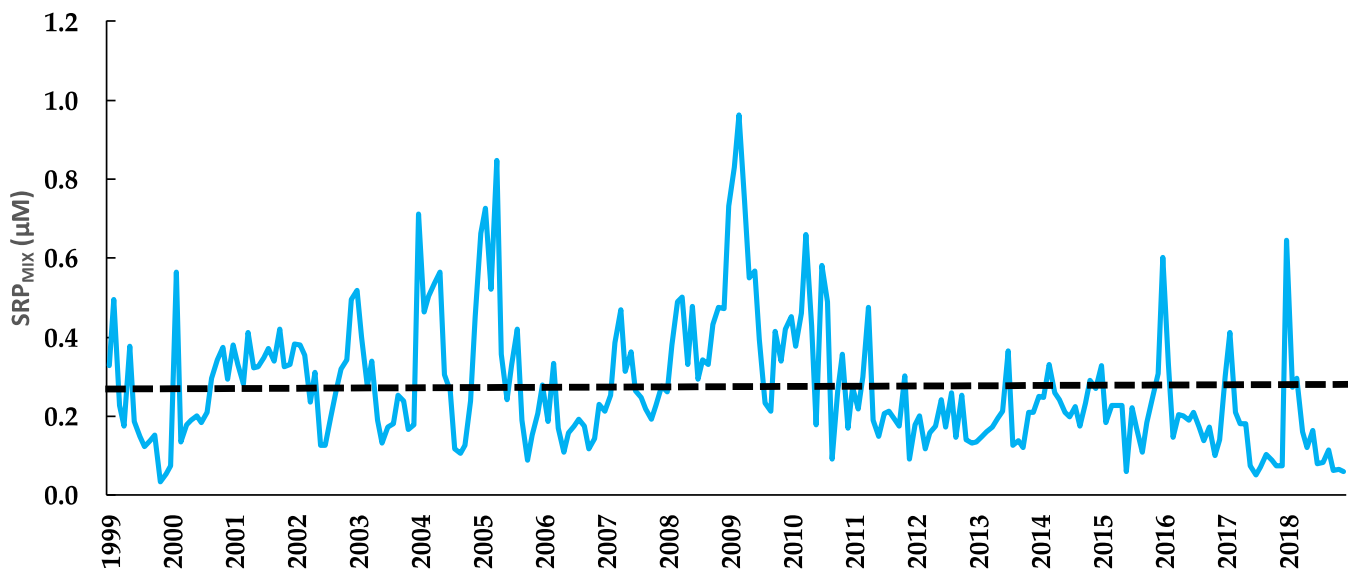


**Figure 14.** Temporal dynamics of the soluble reactive phosphorous concentration in the mixed layer (SRP<sub>MIX</sub>) in Lake Alchichica. (The black dashed line indicates the average SRP<sub>MIX</sub> value from 1998 to 2018).

The SRP<sub>MIX</sub> fluctuated widely interannually (Figure 15). For 40% of the period, the SRP<sub>MIX</sub> was above the annual average, and for 60% was below the annual average. Seasonally, the SRP<sub>MIX</sub> displayed a regular dynamic with two periods (Figure 15). The first was when SRP<sub>MIX</sub> was lower (below the annual average), and most of the stratification (June to December). The second one corresponded to the mixing season and early stratification (January to May) when SRP<sub>MIX</sub> was higher (above the annual average).

### 3.8. Soluble Reactive Silica of the Mixed Layer (SRSi<sub>MIX</sub>)

The soluble reactive silica concentration in the mixed layer (SRSi<sub>MIX</sub>) displayed substantial interannual variability in Lake Alchichica from 1999 to 2018 (Figure 16). There was not a clear annual pattern of the SRSi<sub>MIX</sub> associated with the water column mixing and stratification periods. The SRSi<sub>MIX</sub> annual average was  $4.6 \pm 3.6 \mu\text{M}$  within a range of  $1.9 \pm 1.1 \mu\text{M}$  and  $11.6 \pm 5.2 \mu\text{M}$ .

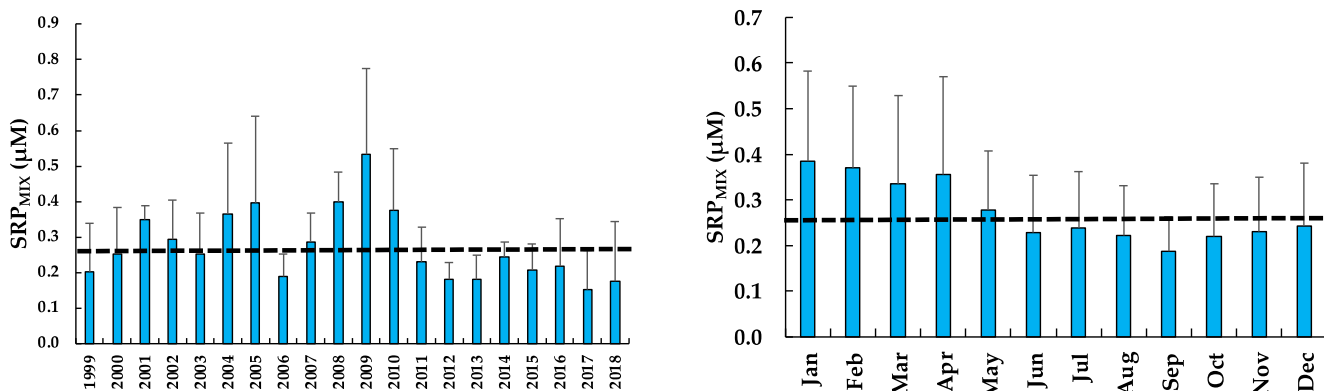


**Figure 15.** Interannual (left) and annual (seasonal) (right) variation in the soluble reactive phosphorous concentration (average  $\pm$  s.d.) in the mixed layer (SRP<sub>MIX</sub>) in Lake Alchichica. (The dashed lines indicate the average SRP<sub>MIX</sub> value from 1998 to 2018).

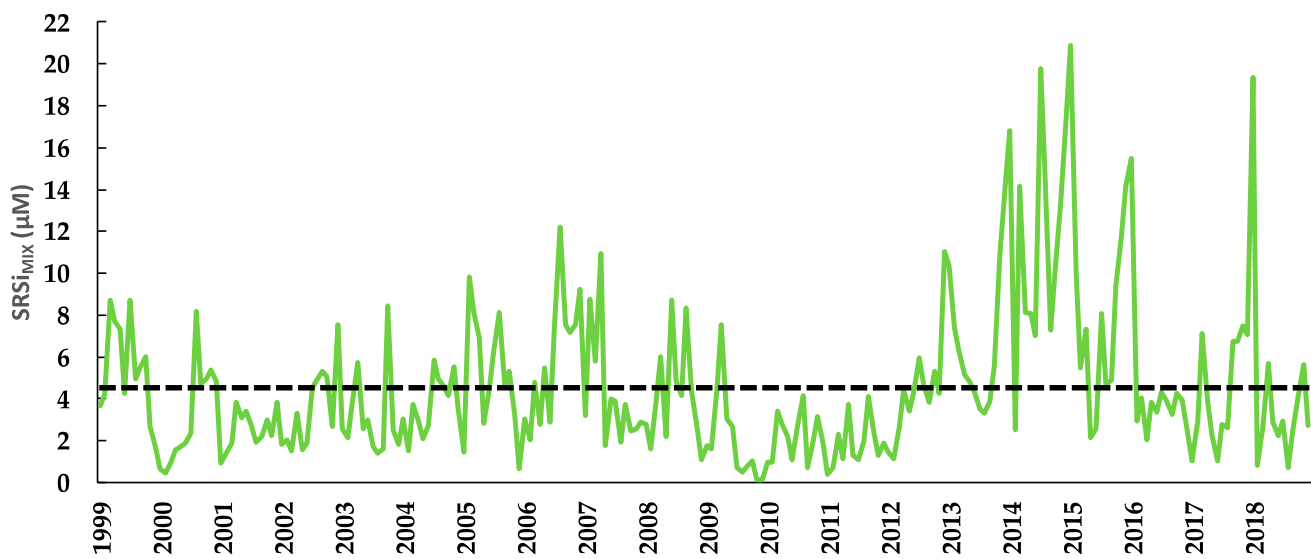


**Figure 16.** Temporal dynamics of the soluble reactive silica concentration in the mixed layer (SRSi<sub>MIX</sub>) in Lake Alchichica. (The black dashed line indicates the average SRSi<sub>MIX</sub> value from 1998 to 2018).

The SRSi<sub>MIX</sub> fluctuated extensively interannually (Figure 17). For 30% of the period, the SRSi<sub>MIX</sub> was above the annual average, and for 70% was below the annual average. The SRSi<sub>MIX</sub> displayed irregular dynamic alternating values below and above the annual average (Figure 17). One-third of the year, SRSi<sub>MIX</sub> was below the annual average (February, May–June, and September). For the rest of the year (January, March–April, July–August, and October–December), the SRSi<sub>MIX</sub> was above the annual average.

### 3.9. Wavelet Analyses

Wavelet analysis was used to decompose the Chl-a variability from 1998 to 2018 as a function of period and time. We examined if the continuous wavelet transforms could successfully identify variability in the annual scale. The local wavelet power spectrum measures the variance distribution of the time series according to time and periodicity; high variability is represented by red color, whereas blue indicates weak variability. The wavelet spectrum showed that Chl-a (Figure 18) displayed a consistent 1-year periodicity from 1998 until 2012. The strength of the annual periodicity changed over time, suggesting a non-stationary behavior of the time series. There was a weakening of the annual periodicity from 2008 to 2012 until it became statistically non-significant from 2013 to 2015. Moreover, a consistent and statistically significant periodicity between ~4 and 5 years in Chl-a was

detected. A semi-annual periodicity was significant for a short time, around 2016, but did not emerge as significant in the global wavelet spectrum. Wavelet analysis of the Multivariate “El Niño Southern Oscillation” (ENSO) Index (MEI) time series (Figure 18) showed a 2-year and a four to five-year periodicity.

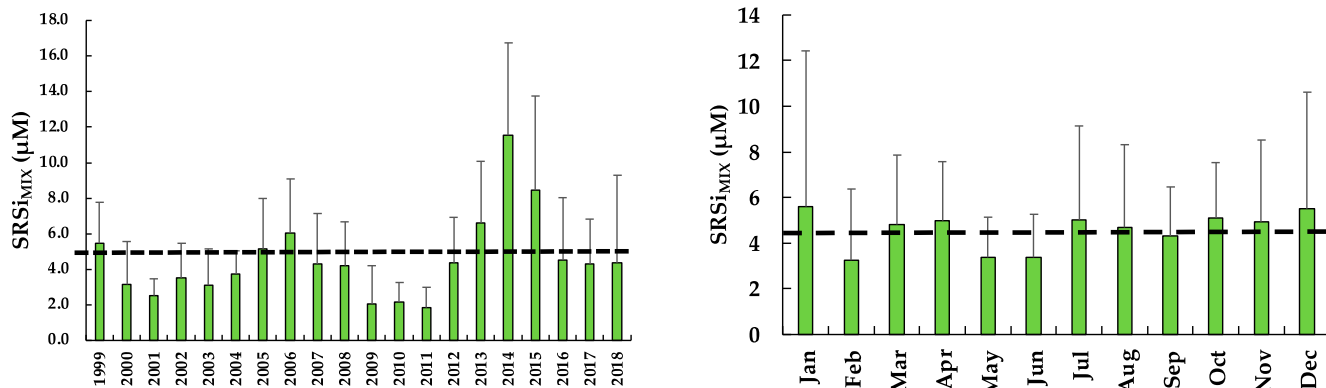


**Figure 17.** Interannual (left) and annual (seasonal) (right) variation in the soluble reactive silica concentration (average  $\pm$  s.d.) in the mixed layer (SRSi<sub>MIX</sub>) in Lake Alchichica. (The dashed lines indicate the average SRSi<sub>MIX</sub> value from 1998 to 2018).

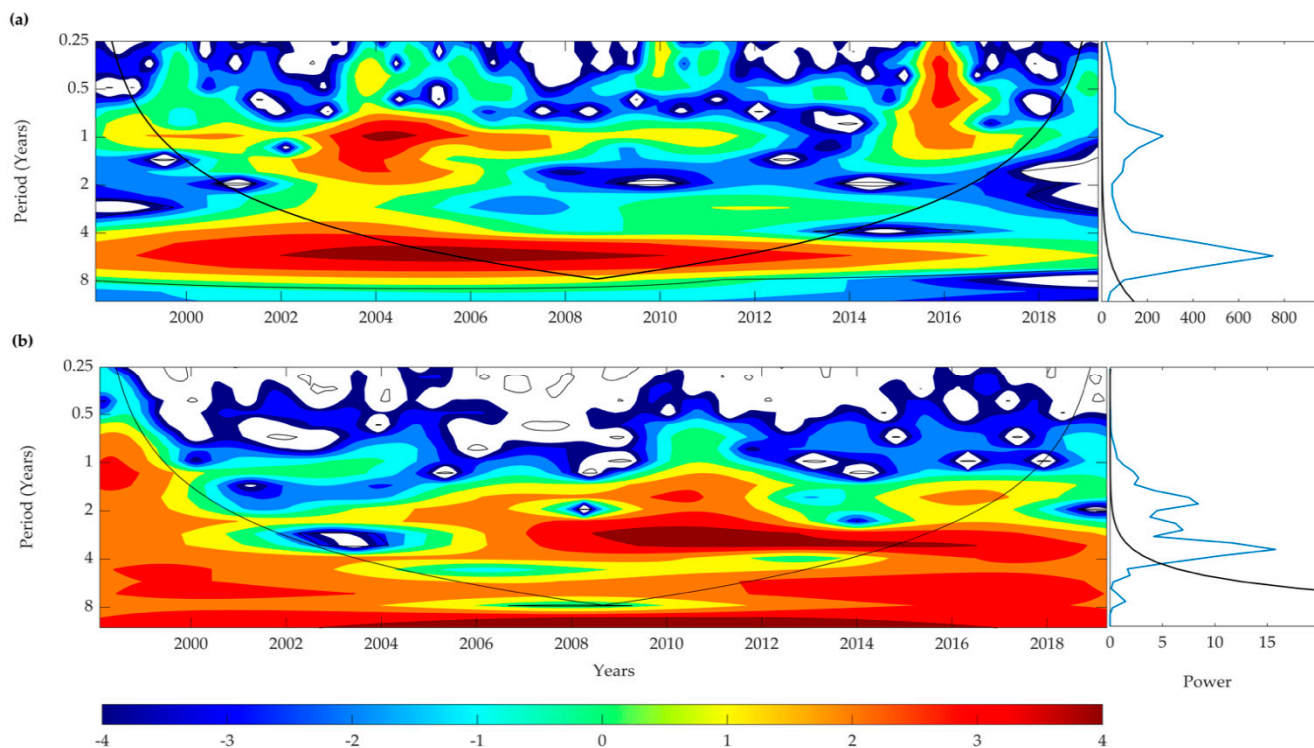


**Figure 18.** Continuous wavelet power spectra showing the periodicity (left) and time-averaged (above global) wavelet power spectra (right) of (a) Chl-a concentration integrated per unit area in Lake Alchichica. Continuous wavelet power spectra showing the periodicity (left) and time-averaged (above global) wavelet power spectra (right) of (b) the Multivariate ENSO Index (MEI) in Lake Alchichica.

However, the former 2-year periodicity showed shifts between 2002 and 2004 and between 2012 and 2015, whereas the latter’s (~4–5 years) period remained stable for the duration of the time series. This shift in periodicity coincides with the shifts in periodicity displayed by the Chl-a wavelet spectrum (Figure 9). Wavelet analysis of the Z<sub>EU</sub>, Z<sub>MIX</sub>, T<sub>MIX</sub>, and DO<sub>MIX</sub> showed stable 1-year periodicities for the whole duration of the time series

(Figure 19). This steady behavior means that the system's complexity has not deteriorated so that the seasonality of this process has not perceptibly changed over time. In addition, a 4-year periodicity was significant for the  $Z_{\text{MIX}}$  time series.

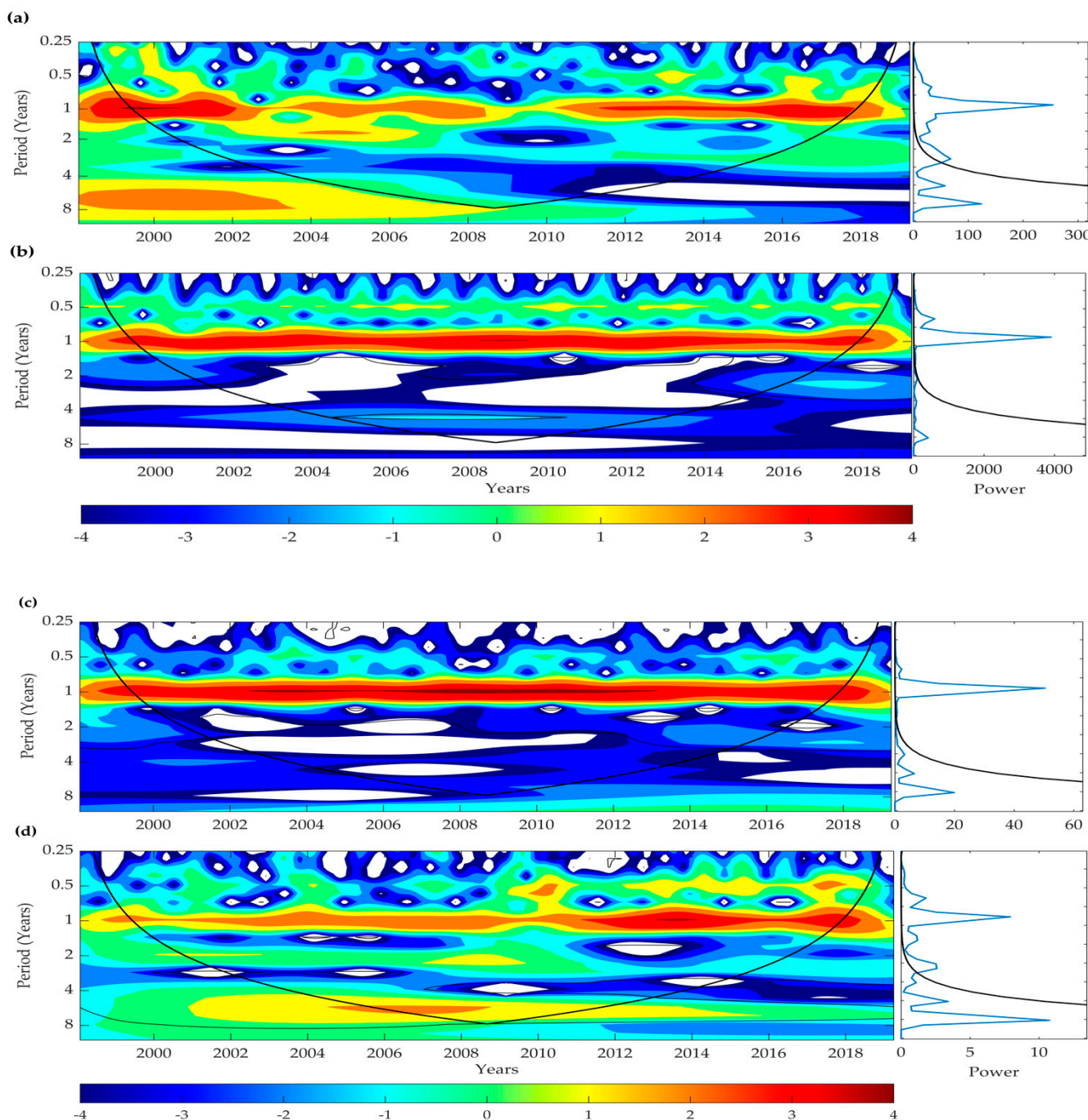


**Figure 19.** Continuous wavelet power spectra showing the periodicity (left) and time-averaged (above global) wavelet power spectra (right) of (a) euphotic zone ( $Z_{\text{EU}}$ ), (b) depth of the mixed layer ( $Z_{\text{MIX}}$ ), (c) temperature of the  $Z_{\text{MIX}}$  ( $T_{\text{MIX}}$ ), and (d) dissolved oxygen concentration of the  $Z_{\text{MIX}}$  ( $\text{DO}_{\text{MIX}}$ ) in Lake Alchichica.

Finally, the wavelet power spectrum for nutrients ( $\text{DIN}_{\text{MIX}}$  = dissolved inorganic nitrogen,  $\text{SRP}_{\text{MIX}}$  = soluble reactive phosphorus,  $\text{SRSi}_{\text{MIX}}$  = soluble reactive silica) also showed statistically significant periodic structures by the annual (1-year) cycle and, in addition, a 2-year and a ~4–5 years statistically significant periodicities were also characterized for the time series (Figure 20).

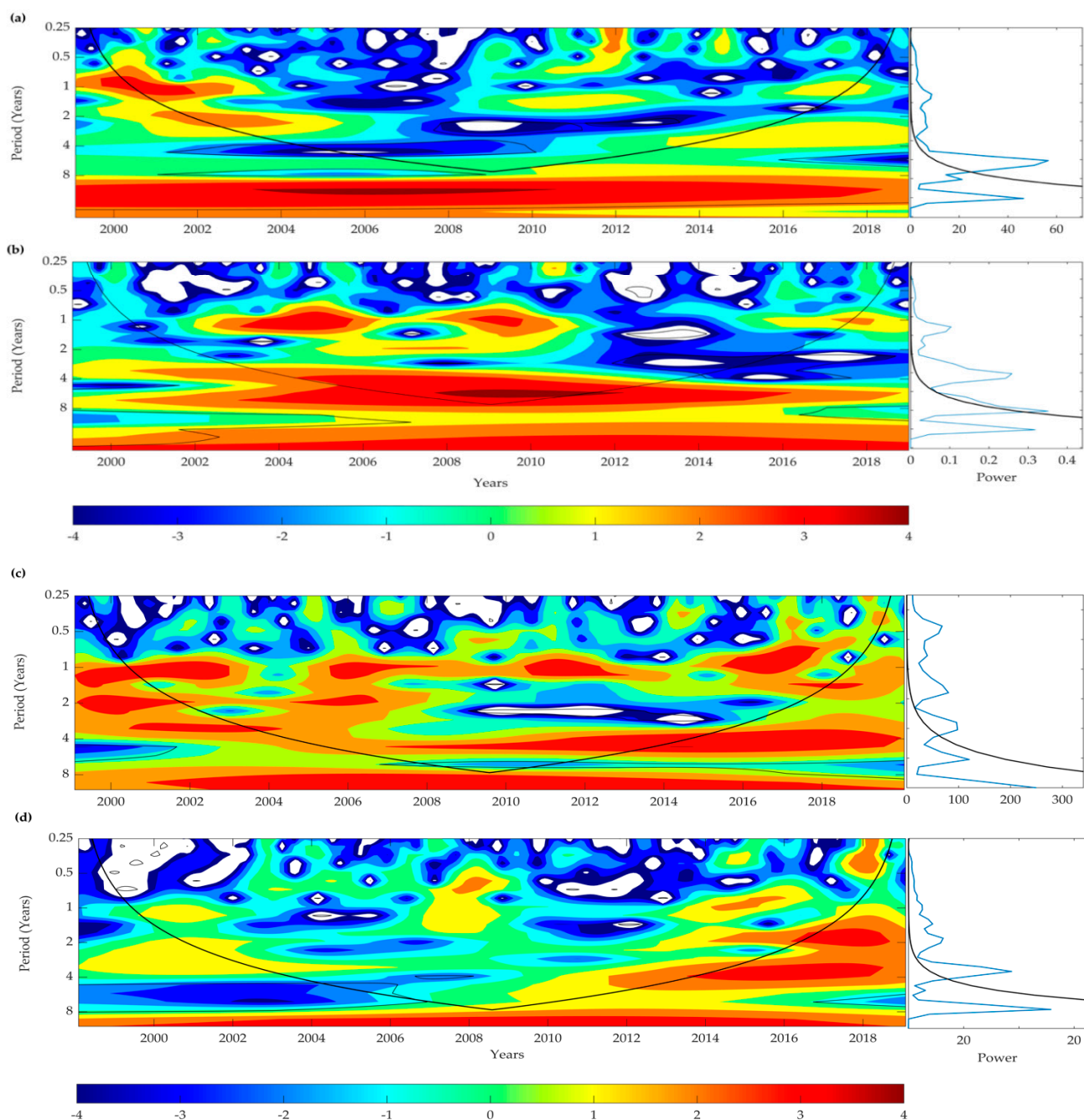


**Figure 20.** Continuous wavelet power spectra showing the periodicity (left) and time-averaged (above global) wavelet power spectra (right) of (a) dissolved inorganic nitrogen concentration ( $\text{DIN}_{\text{MIX}}$ ), (b) soluble reactive phosphorous concentration ( $\text{SRP}_{\text{MIX}}$ ), (c) soluble reactive silica concentration ( $\text{SRSi}_{\text{MIX}}$ ), and (d)  $\text{SRSi}_{\text{MIX}}/\text{DIN}_{\text{MIX}}$  ratio in Lake Alchichica.

All significant scales in the wavelet spectrum were clustered around the 1-year period. However, the power of the annual scale was much lower from 2002 to 2004, except for the SRPMIX time series. Four-year periodicities were statistically significant for most of the nutrient time series. However, the DINMIX time series 2-year periodicity became statistically non-significant after 2005.

#### 4. Discussion

Winder and Cloern [20] found the most common pattern reported in temperate and subtropical aquatic ecosystems, one phytoplankton peak per year or the “canonical spring-

bloom pattern” [5,36], to be less frequent than expected (48%), and although the climate-driven annual cycle is an important driver, other factors can mask it leading to other periodicities or even the lack of periodicity [14]. Melack [1] found that most tropical lakes exhibit seasonal fluctuations associated with rainfall, river discharge, or vertical mixing, corresponding to the hydrological (water input-output) or hydrographic (water column and circulation) features of Talling [10]. Lake Alchichica has no river discharge and lies in a semi-desertic area; then, the seasonality is driven by hydrographic features controlled by its thermal stratification and mixing pattern.

Deep tropical lakes are warm-monomictic, showing great regularity in seasonal mixing, which typically coincides with the hemispheric winter (e.g., [37]). Previous studies on Lake Alchichica suggested the latter (e.g., [22,38,39]) and herein confirmed during the 21 annual cycles studied. Lake Alchichica showed a remarkable regularity on the hydrodynamical pattern (warm monomixis), displaying a predictable annual, complete mixing period in winter (January to March) and remained stratified for the remainder of the year. Adame et al. [3] subdivided the stratification period into three stages: (a) early stratification (April to June) when the thermocline was close to the surface and poorly defined, (b) well-established stratification (July to September) when the water column displays a clear layering (epi, meta, and hypolimnion), and (c) late stratification (October to December) when the thermocline deepened and the metalimnion thinned.

The recurrent annual thermal stratification and mixing pattern of Lake Alchichica and its main limnological features could be summarised as follow (Table 1).  $Z_{MIX}$  is at maximum (from surface down to the bottom) during the mixing season, and the water column is cold and well-oxygenated. Nutrients (DIN, SRP, and SRSi) reach high concentrations along the water column, promoting the winter diatom bloom development, resulting in high Chl-a concentration and the lowest values of  $Z_{EU}$ . The mixing season is the turbid water phase associated with high biogenic turbidity. The winter bloom comprises the centric diatom *Cyclotella alchichicana* [3,26].

**Table 1.** Comparison of the main limnological features of Lake Alchichica during the mixing and stratification seasons. (Chl-a: chlorophyll-a concentration,  $Z_{EU}$ : euphotic zone,  $Z_{MIX}$ : mixed layer,  $T_{MIX}$ : temperature in the  $Z_{MIX}$ ,  $OD_{MIX}$ : dissolved oxygen concentration in the  $Z_{MIX}$ ,  $DIN_{MIX}$ : dissolved inorganic nitrogen in the  $Z_{MIX}$ ,  $SRP_{MIX}$ : soluble reactive phosphorous in the  $Z_{MIX}$ ,  $SRSi_{MIX}$ : soluble reactive silica in the  $Z_{MIX}$ ).

Variable	Mixing (Dry, Cold)	Stratification (Wet, Warm)
Chl-a	High The phytoplankton distributes throughout the water column Lower	High The phytoplankton concentrates at the metalimnion (DCM) Higher
$Z_{EU}$	Turbid water phase Biogenic turbidity	Clear water phase DCM at the bottom of $Z_{EU}$
$Z_{MIX}$	High	Low
$T_{MIX}$	Colder	Warmer
$OD_{MIX}$	Lower	Higher
$DIN_{MIX}$	Higher	Lower
$SRP_{MIX}$	Higher	Lower
$SRSi_{MIX}$	Higher and lower	Higher and lower

At the onset of the stratification period, the warmer and well-lit epilimnion, and nutrient depletion, particularly nitrogen, favored the nitrogen-fixing cyanoprokariota *Nodularia aff. spumigena* to bloom for a brief period [28]. Monthly, nitrogen was the primary productivity limiting nutrient ( $DIN_{MIX}/SRP_{MIX} < 15, 10 \pm 2, 7-14$ ), while interannually, nitrogen was limiting 75% (15 years) and phosphorus 25% (5 years) of the time.

The stratification period corresponds to the clear water phase with high values of  $Z_{EU}$  related to the presence of low Chl-a concentration in the  $Z_{MIX}$ . The  $Z_{MIX}$  remains warm and well-oxygenated. Through the extended stratification season,  $Z_{MIX}$  and  $Z_{EU}$  broaden.

While stratified, nutrients are rapidly depleted in the  $Z_{\text{MIX}}$  and remain so for the remaining of the stratification, explaining the low Chla concentration in the  $Z_{\text{MIX}}$  and the high values of  $Z_{\text{EU}}$ .

The large size of *C. alchichicana* makes it inedible for zooplankton [40,41]. Then most of the diatom bloom is not consumed and incorporated in the food web but instead exported below the thermocline, down to the bottom [42]. A large amount of organic matter deposited into the sediments is partially remineralized by consuming the available dissolved oxygen leading to hypolimnetic anoxia [3], and partially buried and sequestered into the sediments [43]. During the stratification period, the organic matter remineralization explains the nutrient accumulation in the hypolimnion. Along the stratification period, nutrients are depleted in the epilimnion and accumulated in the hypolimnion.

Approximately from September to November, a DCM develops at the metalimnion. The Chl-a concentration at the DCM reaches high values, similar to those recorded in the winter diatom bloom. The DCM is mainly composed of *C. alchichicana*, which is exported below the thermocline down to the sediments [42]. In this way, two Chl-a peaks are recognized in the annual cycle: a diatom winter blooms along the water column during the mixing season. The second is a DCM at the metalimnion in the stratification.

As previously mentioned, Lake Alchichica showed not one but two phytoplankton peaks per year (Figure 21): the winter bloom (Chl-a:  $23 \pm 5 \text{ mg m}^{-2}$ ) and the DCM (Chl-a:  $28 \pm 12 \text{ mg m}^{-2}$ ). The average Chl-a concentration of the mixing period (January to March) was higher than in the DCM in five years (24%), while the Chl-a concentration in the DCM was higher than in the mixing season in sixteen years (76%). The winter diatom bloom duration fluctuated between 1 and 4 months (January–April), with Chl-a concentrations above the 21-year average. January (11, 52.4%) and February (8, 38.1%) were the most representative months of the winter diatom bloom. Differently, in six years (2006–2009 and 2017–2018), the Chl-a concentrations in the diatom bloom were below the average for the whole period. The DCM duration fluctuated between 1 and 5 months (August–December), with Chl-a concentrations above the 21-year average. September and October (14, 66.7%) were the most representative months of the stratification DCM. Contrarily, in two years (2001 and 2011), the Chl-a concentrations in the DCM were below the average for the whole period.

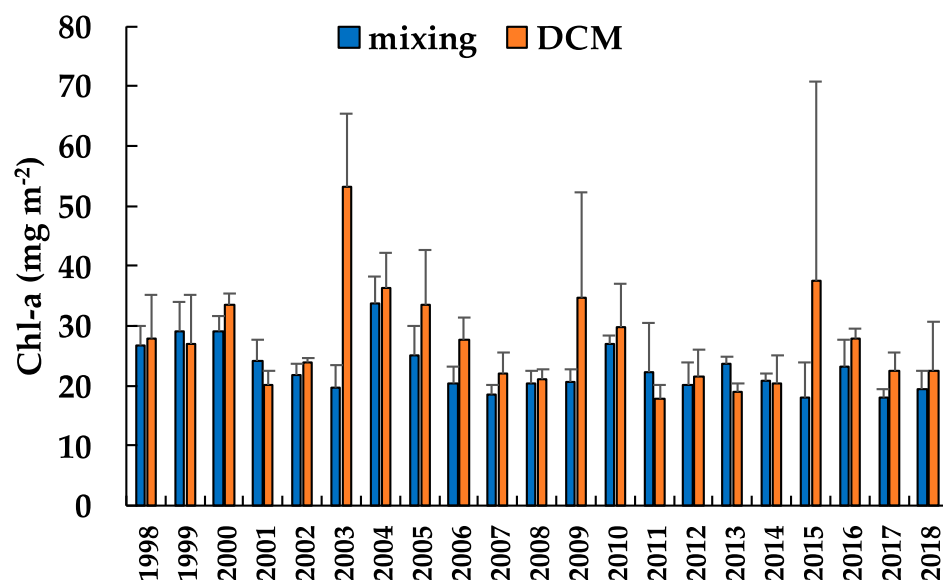


**Figure 21.** Average water-column integrated chlorophyll-a concentration (Chl-a) in Lake Alchichica during the mixing (January–March) and the DCM (September–November).

Lewis [44] compared the phytoplankton biomass in temperate and tropical lakes by analyzing the ratio of annual and seasonal mean to maximum biomass. Tropical lakes

displayed a higher ratio (0.45) of annual mean to maximum than temperate lakes (0.36). However, the ratio of seasonal mean to maximum biomass ( $\sim 0.7$ ) was similar in both tropical and temperate lakes. The latter means the intensity of the annual bloom in both tropical and temperate lakes are similar, but tropical lakes display higher minimum Chl-a concentrations throughout the year. The annual ratio of mean to maximum Chl-a in Lake Alchichica ranged between 0.36 and 0.85 ( $0.68 \pm 0.13$ ), which is higher than those reported by Lewis [44] for tropical lakes (0.39 to 0.58) but similar to the seasonal ratio of mean to maximum Chl-a with 0.65 to 0.80. The discrepancy could be that Lewis [44] calculated the seasonal ratio by considering the 3-month interval with the highest biomass, most likely associated with the winter (mixing) bloom. The seasonal ratio of mean to maximum Chl-a calculated for the winter diatom bloom (3 months, January to March) in Lake Alchichica is 0.62, slightly lower than the seasonal ratio of Lewis [44] with 0.65 to 0.80.

The seasonal ratio of mean to maximum Chl-a calculated for the DCM (4 months, August to November) is 0.36, much lower than the seasonal ratio of Lewis [44] with 0.65 to 0.80. The three largest Chl-a concentration peaks could have biased this low value throughout 21 years, corresponding to the DCM (October 2003, October 2009, September 2015).

The annual variation in phytoplankton biomass in temperate lakes is greater than in tropical lakes [44]. Kalff and Watson [45] found that Lake Naivasha had low and seasonal variable ( $10\times$ ) phytoplankton biomass. Differently, the coefficient of variation in Lake Alchichica annual phytoplankton biomass averages  $27 \pm 14\%$ , and low ( $1.3\times$ ) seasonal variation in biomass (i.e., mixing:  $23 \pm 5 \text{ mg m}^{-2}$ , early stratification:  $19 \pm 4 \text{ mg m}^{-2}$ , well-established stratification:  $25 \pm 10 \text{ mg m}^{-2}$ , and late stratification:  $25 \pm 10 \text{ mg m}^{-2}$ ). There were also interannual differences in the max:min biomass ratio with an average of  $2.4 \pm 1.0$  (1.5 to 6.1). The inter-annual variability of Chl-a was high  $.7\times$ - (annual mean: 18 to  $30 \text{ mg m}^{-2}$ ), similarly to Lake Kivu with  $1.9\times$  [12].

Our analyses showed that continuous wavelet transforms successfully detect the phenology of the Chl-a concentration and associated limnological parameters over time. Throughout the time series, periodicities associated with the annual cycle represented the dominant scale of variation. As mentioned, the recurrent and predictable annual cyclicity is explained mainly by the warm-monomictic thermal pattern of Lake Alchichica, with the water column mixing being the most important driving force explaining the seasonality.

However, the Chl-a continuous wavelet transforms identified a temporary decrease in the strength of the annual periodicity. While the annual periodicity was the most important scale of variation for the Chl-a during 1998–2010, it was significantly weakened from 2011 to 2015, when it became no longer statistically significant. In this period, there were slight decreases ( $Z_{\text{EU}}$ ,  $Z_{\text{MIX}}$ ) and increases ( $T_{\text{MIX}}$ ,  $D_{\text{OMIX}}$ ) in the limnological variables associated with decreases in Chl-a concentration. Interestingly, this shift in periodicity in the Chl-a power spectrum between 2011 and 2015 coincided with intense La Niña events (2011–2012) and with the “Godzilla” El Niño event (2015).

Tropical lakes are particularly sensitive to climate change [46,47]. A previous study [40] reported that the 1998–1999 El Niño resulted in higher epilimnetic temperatures and lower Chl-a concentrations in Lake Alchichica. Recently, Alcocer et al. [40] found that the air temperature in the Lake Alchichica region increased from 1966 to 2018. This variability was correlated positively with the Oceanic Niño Index (ONI), the Pacific Decadal Oscillation index (PDO), and the Atlantic Multidecadal Oscillation index (AMO), and negatively with the Southern Oscillation Index (SOI).  $T_{\text{MIX}}$  temperature displayed an increasing trend associated with the air temperature increase, while Chl-a concentration displayed a decreasing trend (Table 2). Higher temperatures associated with climate change resulted in stronger thermal stratifications, lower  $Z_{\text{MIX}}$ , and lower nutrient concentration availability.  $D_{\text{INMIX}}$  and  $S_{\text{RPMIX}}$  displayed decreasing trends; contradictorily,  $S_{\text{RSiMIX}}$  showed an increasing trend related to the decreasing trend in Chl-a, indicating lower biomass of diatoms and consequently less  $S_{\text{RSi}}$  uptake.

**Table 2.** Mann–Kendall test results for trend analyses of phytoplanktonic chlorophyll-a concentration (1998–2018), water quality (1998–2018), and trophic (1999–2018) variables of Lake Alchichica. (Chl-a: chlorophyll-a concentration,  $Z_{EU}$ : euphotic zone,  $Z_{MIX}$ : mixed layer,  $T_{MIX}$ : temperature in the  $Z_{MIX}$ ,  $OD_{MIX}$ : dissolved oxygen concentration in the  $Z_{MIX}$ ,  $DIN_{MIX}$ : dissolved inorganic nitrogen in the  $Z_{MIX}$ ,  $SRP_{MIX}$ : soluble reactive phosphorous in the  $Z_{MIX}$ ,  $SRSi_{MIX}$ : soluble reactive silica in the  $Z_{MIX}$ ).

Variable	S	Z	P	Trend
Chl-a	−4045	−3.4669	0.00052653	Decreasing
$Z_{EU}$	−1397	−1.0255	0.30513	Non-Significant
$Z_{MIX}$	−1977	−1.4539	0.14599	Non-Significant
$T_{MIX}$	4341	3.1881	0.001432	Increasing
$OD_{MIX}$	6063	4.4531	$8.4643 \times 10^{-6}$	Increasing
$DIN_{MIX}$	−5525	−4.4426	$8.8884 \times 10^{-6}$	Decreasing
$SRP_{MIX}$	−5570	−4.4796	$7.4786 \times 10^{-6}$	Decreasing
$SRSi_{MIX}$	2751	2.212	0.026964	Increasing

Regarding the 2-year and 4-year periodicities revealed through the continuous wavelet transforms analyses, the biennial cycle in the Chl-a concentration was already reported in Adame et al. [3]. Adame et al. [3] reported higher Chl-a concentrations during the winter diatom blooms of even years while lower in odd years. Higher silicate concentration and Si/N ratio in the hypolimnion during the previous late stratification period led to higher diatom blooms in the following mixing period. Herein, we confirmed the biennial (2-year) cyclicity and provided a plausible explanation of the role silicate and the Si/N ratio play in controlling the phytoplankton biomass in Lake Alchichica.

As mentioned before, the large size of *C. alchichicana* makes it inedible for zooplankton. Then most of the biomass is exported below the thermocline down to the sediments [27]. *C. alchichicana* contributes 98% to the silica flux down to the sediments in Lake Alchichica with  $147 \text{ g m}^{-2} \text{ year}^{-1}$  [42]. Oseguera et al. [48] found the particles captured in sediment traps deployed in Lake Alchichica evaluating exportation into the deep sediments were biogenic, primarily composed of cells of *C. alchichicana*.

Alcocer et al. [43] found high preservation of biogenic carbon—and associated diatom silica—in the deep sediments of Lake Alchichica, suggesting a net carbon and silica lost out of the system. Lake Alchichica, with a low silica concentration availability and phytoplankton biomass dominated by large diatoms, deep, thorough mixing events are crucial for silica mineralization and recycling instead of sequestering. Mineralization and mixing events also replenish the lake with nitrogen which often limits phytoplankton in tropical lakes [49], as in Lake Alchichica [25,50], confirmed by the recurrent annual bloom of *N. aff. spumigena* [28], a nitrogen-fixing cyanobacteria [51].

Climate variability leads to warmer temperatures, which increase the length and strength of thermal stratification (e.g., [52]), preventing nutrient mineralization and recycling. Opposite, colder temperatures favor complete water column mixing and re-oxygenation, favoring nutrient mineralization and recycling, which brought an increased supply of phosphorus and, more importantly, nitrogen which later controlled phytoplankton growth in the  $Z_{EU}$ .

Moreover, there was a ~4–5 years periodicity evidenced in nutrient concentration. We think these 2-year and ~4–5 years periodicities could be associated with ENSO events encompassing stronger winds and then more profound, more complete mixing seasons providing higher nutrient concentrations stimulating larger blooms as suggested by Alcocer et al. [40].

## 5. Conclusions

This work confirmed that wavelet analysis could help us interpret multi-scale, non-stationary time-series data to reveal features that could not otherwise be seen. By using a long-term (1998–2018) limnological database of the tropical, saline Lake Alchichica, we (a) verified the regularity of the annual cycle of the phytoplankton Chl-a associated with the warm-monomictic thermal-mixing-pattern, (b) revealed the phenology of the annual

Chl-a cycle showing large inter-annual variability, (c) identified the presence of a biennial cycle most likely controlled through SRSi availability and Si/N ratio associated to climate variability influencing the length and strength of the annual thermal stratification, and (d) recognize other cycles with different periodicities associated with external forcing agents (e.g., ENSO-El Niño Southern Oscillation). The water quality variables were regular along the 21 years, displaying a recurrent annual pattern. Nutrient concentration, as trophic indicators, revealed the same cyclicity (1-year, 2-year, and ~4–5 years) as Chl-a, suggesting the external forcing agents lead to deeper, more complete mixing events increasing nutrient availability, which in turn stimulate larger Chl-a concentrations.

**Author Contributions:** Conceptualisation, J.A. and L.A.O.; data curation, J.A., B.Q.-M., M.M.-I., L.A.O. and M.M.; formal analysis, J.A., B.Q.-M., M.M.-I., L.A.O. and M.M.; funding acquisition, J.A.; investigation, J.A., B.Q.-M. and L.A.O.; methodology, J.A., B.Q.-M., M.M.-I., L.A.O. and M.M.; project administration, L.A.O.; resources, J.A. and M.M.; software, B.Q.-M.; supervision, J.A., B.Q.-M. and L.A.O.; validation, J.A., B.Q.-M. and L.A.O.; visualization, J.A. and B.Q.-M.; writing—original draft, J.A., B.Q.-M., M.M.-I., L.A.O. and M.M.; writing—review and editing, J.A., B.Q.-M., M.M.-I., L.A.O. and M.M. All authors have read and agreed to the published version of the manuscript.

**Funding:** This research was funded by CONACYT through the projects 0956-N9111, 25430-T, 34893-T, 41667, 49923, 103332, and 224893, the Universidad Nacional Autónoma de México DGAPA/PAPIIT through the projects IN204597, IN210806, IN221009, IN215512, IN219220, and IN231820, by Programa de Investigación en Cambio Climático (PINCC 2012–2014, 2020–2021), and by Project ICML, UNAM 628 (Laboratorio de Ecología Numérica y Análisis de Datos).

**Institutional Review Board Statement:** Not applicable.

**Informed Consent Statement:** Not applicable.

**Data Availability Statement:** Data are available from the authors upon reasonable request.

**Acknowledgments:** We acknowledge Fermín S. Castillo-Sandoval for his technical support with the analysis of nutrients. We thank Mariana Vargas for drawing Figure 1. We are grateful to the anonymous reviewers whose positive and encouraging comments and suggestions greatly improved this paper.

**Conflicts of Interest:** The authors certify that they have no affiliations with or involvement in any organisation or entity with any financial interest (such as honoraria; educational grants; participation in speakers' bureaus; membership, employment, consultancies, stock ownership, or other equity interest; expert testimony or patent-licensing arrangements) or non-financial interest (such as personal or professional relationships, affiliations, knowledge or beliefs) in the subject matter or materials discussed in this manuscript.

## References

1. Melack, J.M. Primary productivity and fish yields in tropical lakes. *Trans. Am. Fish. Soc.* **1976**, *105*, 575–580. [[CrossRef](#)]
2. Field, C.B.; Behrenfeld, M.J.; Randerson, J.T.; Falkowski, P. Primary production of the biosphere: Integrating terrestrial and oceanic components. *Science* **1998**, *281*, 237–242. [[CrossRef](#)]
3. Adame, M.F.; Alcocer, J.; Escobar, E. Size-fractionated phytoplankton biomass and its implications for the dynamics of an oligotrophic tropical lake. *Freshw. Biol.* **2008**, *53*, 22–31. [[CrossRef](#)]
4. Talling, J.F.; Lemoalle, J. *Ecological Dynamics of Tropical Inland Waters*; Cambridge University Press: Cambridge, UK, 1998; p. 452.
5. Sommer, U.; Gliwicz, Z.M.; Lampert, W.; Duncan, A. The PEG-model of seasonal succession of planktonic events in freshwaters. *Arch. Fis. Hydrobiol.* **1986**, *106*, 433–471.
6. Sommer, U.; Adrian, R.; De Senerpont Domis, L.; Elser, J.J.; Gaedke, U.; Ibelings, B.; Jeppesen, E.; Lürling, M.; Molinero, J.C.; Mooij, W.M.; et al. Beyond the Plankton Ecology Group (PEG) model: Mechanisms driving plankton succession. *Annu. Rev. Ecol. Evol. Syst.* **2012**, *43*, 429–448. [[CrossRef](#)]
7. Carey, C.C.; Hanson, P.C.; Lathrop, R.C.; St. Amand, A.L. Using wavelet analyses to examine variability in phytoplankton seasonal succession and annual periodicity. *J. Plankton Res.* **2016**, *38*, 27–40. [[CrossRef](#)]
8. Sarmento, H. New paradigms in tropical limnology: The importance of the microbial food web. *Hydrobiologia* **2012**, *686*, 1–14. [[CrossRef](#)]
9. Plisnier, P.D.; Nshombo, M.; Mgana, H.; Ntakimazi, G. Monitoring climate change and anthropogenic pressure at Lake Tanganyika. *J. Great Lakes Res.* **2018**, *44*, 1194–1208. [[CrossRef](#)]
10. Talling, J.F. The seasonality of phytoplankton in African lakes. *Hydrobiologia* **1986**, *138*, 138–160. [[CrossRef](#)]

11. Lewis, W.M.J. Phytoplankton succession in Lake Valencia, Venezuela. *Hydrobiologia* **1986**, *138*, 189–203. [[CrossRef](#)]
12. Darchambeau, F.; Sarmento, H.; Descy, J.-P. Primary production in a tropical large lake: The role of phytoplankton composition. *Sci. Total Environ.* **2014**, *473–474*, 178–188. [[CrossRef](#)]
13. Kilham, P.; Kilham, S.S. Endless summer: Internal loading processes dominate nutrient cycling in tropical lakes. *Freshwater Biol.* **1990**, *23*, 379–389. [[CrossRef](#)]
14. Rugema, E.; Darchambeau, F.; Sarmento, H.; Stoyneva-Gärtner, M.; Leitao, M.; Thiery, W.; Latli, A.; Descy, J.P. Long-term change of phytoplankton in Lake Kivu: The rise of the greens. *Freshw. Biol.* **2019**, *64*, 1940–1955. [[CrossRef](#)]
15. Cloern, J.E.; Jassby, A.D. Complex seasonal patterns of primary producers at the land–sea interface. *Ecol. Lett.* **2008**, *11*, 1294–1303. [[CrossRef](#)]
16. Paerl, H.W.; Huisman, J. Blooms like it hot. *Science* **2008**, *320*, 57–58. [[CrossRef](#)]
17. Garcia-Soto, C.; Pingree, R.D. Spring and summer blooms of phytoplankton (SeaWiFS/MODIS) along a ferry line in the Bay of Biscay and western English Channel. *Cont. Shelf Res.* **2009**, *29*, 111–1122. [[CrossRef](#)]
18. Cloern, J.E.; Jassby, A.D. Patterns and scales of phytoplankton variability in estuarine–coastal ecosystems. *Estuaries Coasts* **2010**, *33*, 230–241. [[CrossRef](#)]
19. Smayda, T.J. Patterns of variability characterizing marine phytoplankton, with examples from Narragansett Bay. *ICES J. Mar. Sci.* **1998**, *55*, 562–573. [[CrossRef](#)]
20. Winder, M.; Cloern, J.E. The annual cycles of phytoplankton biomass. *Philos. Trans. R. Soc. B* **2010**, *365*, 230–241. [[CrossRef](#)]
21. Mallat, S. *A Wavelet Tour of Signal Processing*; Academic Press: San Diego, CA, USA, 1998; p. 832.
22. Alcocer, J.; Lugo, A.; Escobar, E.; Sánchez, M.R.; Vilaclara, G. Water column stratification and its implications in the tropical warm monomictic Lake Alchichica, Puebla, Mexico. *Verh. des Int. Ver. Limnol.* **2000**, *27*, 3166–3169. [[CrossRef](#)]
23. Filonov, A.; Tereshchenko, I.; Barba-Lopez, M.R.; Alcocer, J.; Ladah, L. Meteorological regime, local climate, and hydrodynamics of Lake Alchichica. In *Lake Alchichica Limnology—The Uniqueness of a Tropical Maar Lake*; Alcocer, J., Ed.; Springer: Cham, Switzerland, 2022; pp. 75–99.
24. Silva-Aguilera, R.A.; Vilaclara, G.; Armienta, M.A.; Escolero, O. Hydrogeology and hydrochemistry of the Serdán-Oriental basin and the Lake Alchichica. In *Lake Alchichica Limnology—The Uniqueness of a Tropical Maar Lake*; Alcocer, J., Ed.; Springer: Cham, Switzerland, 2022.
25. Ramírez-Olvera, M.A.; Alcocer, J.; Merino-Ibarra, M.; Lugo, A. Nutrient limitation in a tropical saline lake: A microcosm experiment. *Hydrobiologia* **2009**, *626*, 5–13. [[CrossRef](#)]
26. Oliva, M.G.; Lugo, A.; Alcocer, J.; Peralta, L.; Sánchez, M.R. Phytoplankton dynamics in a deep, tropical, hypersaline lake. *Hydrobiologia* **2001**, *446*, 299–306. [[CrossRef](#)]
27. Vilaclara, G.; Oliva-Martínez, M.G.; Macek, M.; Ortega-Mayagoitia, E.; Alcántara-Hernández, R.J.; López-Vázquez, C. Phytoplankton of Alchichica: A unique community for an oligotrophic lake. In *Lake Alchichica Limnology—The Uniqueness of a Tropical Maar Lake*; Alcocer, J., Ed.; Springer: Cham, Switzerland, 2022; pp. 192–211.
28. Oliva, M.G.; Lugo, A.; Alcocer, J.; Peralta, L.; Oseguera, L.A. Planktonic bloom-forming *Nodularia* in the saline Lake Alchichica, Mexico. In *Saline Lakes Around the World: Unique Systems with Unique Values*; Oren, A., Naftz, D.L., Wurtsbaugh, W.A., Eds.; The S.J. and Jessie E. Quinney Natural Resources Research Library, College Of Natural Resources, Utah State University: Logan, UT, USA, 2009; pp. 121–126.
29. Keifer, D.A.; Chamberlain, W.S.; Booth, C.R. Natural fluorescence of chlorophyll a: Relationship to photosynthesis and chlorophyll concentration in the western South Pacific gyre. *Limnol. Oceanogr.* **1989**, *34*, 868–881. [[CrossRef](#)]
30. Chamberlain, W.S.; Booth, C.R.; Keifer, D.A.; Morrow, J.H.; Murphy, R.C. Evidence for a simple relationship between natural fluorescence, photosynthesis and chlorophyll in the sea. *Deep-Sea Res.* **1990**, *37*, 951–973. [[CrossRef](#)]
31. Hansen, H.P.; Koroleff, F. Determination of nutrients. In *Methods of Seawater Analysis*; Grasshoff, K., Kremling, K., Ehrhardt, M., Eds.; Wiley-Verlag: Weinheim, Germany, 1999; pp. 159–228.
32. R Development Core Team. *R: A Language and Environment for Statistical Computing*; R Foundation for Statistical Computing: Vienna, Austria, 2020; Available online: <https://www.R-project.org/> (accessed on 6 August 2021).
33. Percival, D.B.; Walden, A.T. *Wavelet Methods for Time Series Analysis*; Cambridge University Press: Cambridge, UK, 2000.
34. Ruffinatti, F.A.; Lovisolo, D.; Distasi, C.; Ariano, P.; Erriquez, J.; Ferraro, M. Calcium signals: Analysis in time and frequency domains. *J. Neurosci. Methods* **2011**, *199*, 310–320. [[CrossRef](#)]
35. Torrence, C.; Compo, G.P. A practical guide to wavelet analysis. *Bull. Am. Meteorol. Soc.* **1998**, *79*, 61–78. [[CrossRef](#)]
36. Cushing, D.H. The seasonal variation in oceanic production as a problem in population dynamics. *ICES J. Mar. Sci.* **1959**, *24*, 455–464. [[CrossRef](#)]
37. Lewis, W.M., Jr. Tropical lakes: How latitude makes a difference. In *Perspectives in Tropical Limnology*; Schiemer, F., Boland, K.T., Eds.; SPB Academic Publishing: Amsterdam, The Netherlands, 1996; pp. 43–64.
38. Cuevas-Lara, J.D.; Alcocer, J.; Oseguera, L.A.; Quiroz-Martínez, B. Dinámica Largo Plazo (1999–2014) de la Productividad Primaria Fitoplancótica en el Lago Alchichica, Puebla. In *Estado Actual del Conocimiento del Ciclo del Carbono y sus Interacciones en México: Síntesis a 2016*; Paz Pellat, F., Wong González, J., Torres Alamilla, R., Eds.; Serie Síntesis Nacionales; Programa Mexicano del Carbono en colaboración con la Universidad Autónoma del Estado de Hidalgo: Texcoco, México, 2016; p. 732.
39. González Contreras, C.G.; Alcocer, J.; Oseguera, L.A. Clorofila a fitoplancótica en el lago tropical profundo Alchichica: Un registro de largo plazo (1999–2010). *Hidrobiológica* **2015**, *25*, 347–356.

40. Alcocer, J.; Lugo, A.; Fernández, R.; Vilaclara, G.; Oliva, M.G.; Osegueda, L.A.; Silva-Aguilera, R.A.; Escolero, Ó. 20 years of global change on the limnology and plankton of a tropical, high-altitude lake. *Diversity* **2022**, *14*, 190. [[CrossRef](#)]
41. Fernández, R.; Alcocer, J.; Lugo, A.; Osegueda, L.A.; Guadarrama-Hernández, S. Seasonal and interannual dynamics of pelagic rotifers in a tropical, saline, deep lake. *Diversity* **2022**, *14*, 113. [[CrossRef](#)]
42. Ardiles, V.; Alcocer, J.; Vilaclara, G.; Osegueda, L.A.; Velasco, L. Diatom fluxes in a tropical, oligotrophic lake dominated by large-sized phytoplankton. *Hydrobiologia* **2012**, *679*, 77–90. [[CrossRef](#)]
43. Alcocer, J.; Ruiz-Fernández, R.; Escobar, E.; Pérez-Bernal, L.H.; Osegueda, L.A.; Ardiles-Gloria, V. Deposition, burial and sequestration of carbon in an oligotrophic, tropical lake. *J. Limnol.* **2014**, *72*, 223–235. [[CrossRef](#)]
44. Lewis, W.M., Jr. Comparisons of phytoplankton biomass in temperate and tropical lakes. *Limnol. Oceanogr.* **1990**, *35*, 1838–1845. [[CrossRef](#)]
45. Kalff, J.; Watson, S. Phytoplankton and its dynamics in two tropical lakes: A tropical and temperate zone comparison. *Hydrobiologia* **1986**, *138*, 161–176. [[CrossRef](#)]
46. Descy, J.P.; Sarmento, H. Microorganisms of the East African Great Lakes and their response to environmental changes. *Freshw. Rev.* **2008**, *1*, 59–73. [[CrossRef](#)]
47. Kraemer, B.M.; Pilla, R.M.; Woolway, R.I.; Anneville, O.; Ban, S.; Colom-Montero, W.; Devlin, S.P.; Dokulil, M.T.; Gaiser, E.E.; Hambricht, K.D.; et al. Climate change drives widespread shifts in lake thermal habitat. *Nat. Clim. Change* **2021**, *11*, 521–529. [[CrossRef](#)]
48. Osegueda, L.A.; Alcocer, J.; Vilaclara, G. Relative importance of dust inputs and aquatic biological production as sources of lake sediments in an oligotrophic lake in a semi-arid area. *Earth Surf. Process. Landf.* **2011**, *3*, 419–426. [[CrossRef](#)]
49. Lewis, W.M., Jr. Causes for the high frequency of nitrogen limitation in tropical lakes. *Verh. des Int. Ver. Limnol.* **2002**, *28*, 210–213. [[CrossRef](#)]
50. Ramos-Higuera, E.; Alcocer, J.; Ortega-Mayagoitia, E.; Camacho, A. Nitrógeno: Elemento limitante para el crecimiento fitoplanctónico en un lago oligotrófico tropical. *Hidrobiológica* **2008**, *18*, 105–113.
51. Falcón, L.I.; Escobar-Briones, E.; Romero, D. Nitrogen fixation patterns displayed by cyanobacterial consortia in Alchichica crater-lake, Mexico. *Hydrobiologia* **2002**, *467*, 71–78. [[CrossRef](#)]
52. Butcher, J.B.; Nover, D.; Johnson, T.E.; Clark, C.M. Sensitivity of lake thermal and mixing dynamics to climate change. *Clim. Chang.* **2015**, *129*, 295–305. [[CrossRef](#)]